UCRL 9880

University of California

Ernest O. Lawrence Radiation Laboratory

HEAT-CAPACITY STUDIES AT LIQUID HELIUM TEMPERATURES AND BELOW
PART I: THE ALKALI METALS
PART II: SMALL PARTICLES OF MAGNESIUM OXIDE

Berkeley, California

DISCLAIMER

This document was prepared as an account of work sponsored by the United States Government. While this document is believed to contain correct information, neither the United States Government nor any agency thereof, nor the Regents of the University of California, nor any of their employees, makes any warranty, express or implied, or assumes any legal responsibility for the accuracy, completeness, or usefulness of any information, apparatus, product, or process disclosed, or represents that its use would not infringe privately owned rights. Reference herein to any specific commercial product, process, or service by its trade name, trademark, manufacturer, or otherwise, does not necessarily constitute or imply its endorsement, recommendation, or favoring by the United States Government or any agency thereof, or the Regents of the University of California. The views and opinions of authors expressed herein do not necessarily state or reflect those of the United States Government or any agency thereof or the Regents of the University of California.

UCRL-9880
UC-4 Chemistry
TID-4500 (16th Ed.)

UNIVERSITY OF CALIFORNIA

Lawrence Radiation Laboratory

Berkeley, California

Contract No. W-7405-eng-48

HEAT-CAPACITY STUDIES AT LIQUID HELIUM TEMPERATURES AND BELOW

PART I: THE ALKALI METALS

PART II: SMALL PARTICLES OF MAGNESIUM OXIDE

William Henry Lien

(Ph.D. Thesis)

January 1962

Printed in USA. Price $2.00. Available from the
Office of Technical Services
U. S. Department of Commerce
Washington 25, D.C.

HEAT-CAPACITY STUDIES AT LIQUID HELIUM TEMPERATURES AND BELOW

Contents

Abstract v

PART I: THE ALKALI METALS

I. Experimental Aspects

A. Introduction 1

B. The Apparatus 2

C. Procedures 9

II. Heat Capacity of Sodium, Potassium, Rubidium, and Cesium

A. Introduction 13

B. Results 17

C. Discussion 40

1. Sodium 40

2. Electronic Heat Capacity 41

3. Lattice Heat Capacity 45

D. Conclusion 52

PART II: SMALL PARTICLES OF MAGNESIUM OXIDE

I. Heat Capacity of Small Particles of Magnesium Oxide

A. Introduction 53

B. Results 57

C. Discussion 63

Acknowledgments 66

Appendix: Heat-Capacity Anomaly in Solid Air 67

References 70

HEAT-CAPACITY STUDIES AT LIQUID HELIUM TEMPERATURES AND BELOW

PART I: THE ALKALI METALS

PART II: SMALL PARTICLES OF MAGNESIUM OXIDE

William Henry Lien

Lawrence Radiation Laboratory
University of California
Berkeley, California

January 1961

ABSTRACT

The heat capacity of sodium was measured from 0.15 to 1.5 $^{\circ}$K and that of potassium, rubidium, and cesium from 0.15 to 4.0°K. Their heat capacities could be represented by $\gamma T + AT^3 + BT^5$ for $T < \theta/30$, where γT represents the contribution of the conduction electrons, and $AT^3 + BT^5$ represents the contribution of the lattice vibrations. For each metal, γ was compared with values given by various theories of the electronic structure of metals. Also for each metal, A and B were compared with the results of a lattice dynamic calculation.

The heat capacity of two samples of two samples of magnesium oxide powder was measured from 1.5 through 4.0°K. One sample had a specific surface area of 166 m^2/g and the other, 13.1 m^2/g. The heat capacity of both samples could be represented by the sum of a T^2 and a T^3 term. The T^3 term is the usual volume-dependent term representing the total heat capacity in a macrocrystalline sample. The T^2 term is surface-dependent term and appears only in samples with high surface-to-volume ratios. This term was compared with various theories of surface heat capacities for both samples.

I. EXPERIMENTAL ASPECTS

A. Introduction

The heat capacity of a specimen is defined by

$$C\ (T) = \lim_{\Delta T \to 0} (\Delta Q/\Delta T), \tag{1}$$

and so can be obtained directly be measuring the temperature increase that results from the addition of a known quantity of heat. The method for determining heat capacity introduced by Nernst[1] and Eucken[2] has been used in nearly all low-temperature calorimetric work. In this method, a calorimeter containing the sample under investigation is isolated from its surroundings by means of a high vacuum, and the temperature-rise ΔT resulting from the introduction of a known quantity of heat ΔQ is measured. The calorimeter thus consists of the sample and certain addenda; namely, everything that is in good thermal contact with the sample during the calorimetric measurements. The primary measurements yield the heat capacity of the calorimeter only, so that it is necessary to determine that of the addenda separately to obtain the heat capacity of the sample.

In Sec. I-B, an apparatus for determining heat capacity by this method at liquid helium temperatures and below is described, and in Sec. I-C, procedures involved in making the measurements are set forth.

B. The Apparatus

Figure 1 shows the apparatus as set up for measurements at temperatures below those obtainable with liquid helium. Temperatures between 1.1 ^{o}K and 0.1 ^{o}K were obtained by the adiabatic demagnetization of copper potassium sulfate. Thermal contact with the salt pill was made by molding the powdered salt under pressure onto a system of thin copper vanes attached to a copper wire. The copper wire was soldered to a copper tube; this provided a thermal shield at the same temperature as the paramagnetic salt. The salt pill was supported by a Lucite tube mounted on the bottom of the copper tube. The calorimeter was rigidly supported by cotton threads inside the copper shield. The copper shield was likewise rigidly supported by cotton threads inside a brass cage attached to the bottom of the vapor-pressure thermometer. The brass cage was surrounded by a vacuum-tight brass can connected to the vapor-pressure thermometer by a soft-solder joint. The space containing the salt pill and calorimeter was evacuated by an oil diffusion pump to a pressure of the order of 10^{-6} mm of Hg, as measured with an untrapped ionization gauge at room temperature. After reaching liquid helium temperatures, however, this space was completely closed off, to eliminate heat input from radiation or from hot gas molecules entering through the pumping tube. The electrical leads were introduced through glass-Kovar seals, the wire for operating the mechanical heat switch was sealed to the vacuum jacket with a flexible metal bellows, and the pumping tube was closed at its lower end by the action of a metal plunger.

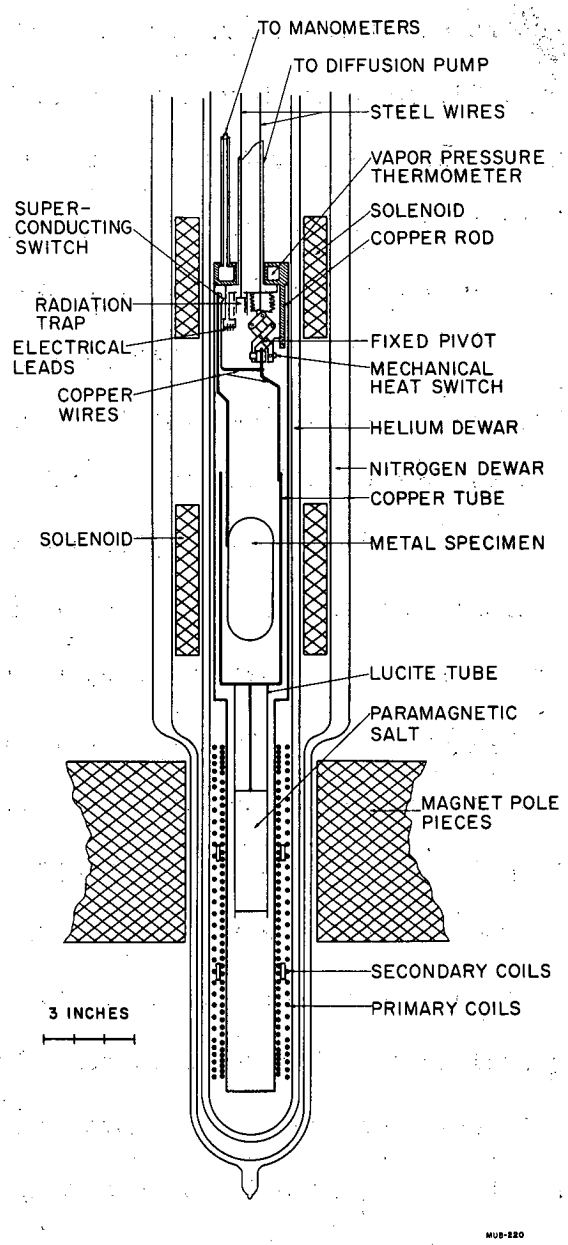

Fig. 1. The apparatus.

Thermal contact between the calorimeter and the salt pill was controlled by a superconducting thermal switch. The switch consisted of a 20-cm length of 0.031-in.-diam lead wire connecting two copper wires, one soldered to the copper shield and the other soldered to the calorimeter. The lead wire has a very hight thermal resistance when in the superconducting state, but a very low one when brought into the normal state by a magnetic field. The lead wire was positioned as far from the calorimeter as possible, to reduce the eddy current heating induced in the calorimeter by the change in the magnetic field of the solenoid operating the switch.

Thermal contact between the salt pill and the bulb of the vapor pressure thermometer was made or broken by closing or opening a mechanical heat switch. The switch comprised two copper jaws, connected to the vapor pressure bulb by flexible copper wires, that could be closed on a central copper wire soldered to the copper shield. The jaws were normally held open by a spring and were closed by a system of levers actuated by applying tension to a steel wire that passed through the pumping tube to an adjusting screw at the top of the cryostat.

The mechanical heat switch has a number of advantages over the helium-exchange gas, which it replaces. It removes a major source of heat leak, namely gas conduction, and it eliminates errors associated with the desorption of adsorbed helium during a heating period. In addition, the switch makes it possible to extend the measurements to 1.3 $^{\circ}$K, through the temperature range in which outgassing of the adsorbed helium from the salt pill would otherwise spoil the insulating vacuum.

All electrical leads were placed in thermal contact with the copper shield before being led to the calorimeter. Between the glass-Kovar seals

at the bottom of the pumping tube and the copper shield, and also between the shield and the calorimeter, the leads consisted of 20-cm. lengths of 0.0015-in.-diam Manganin wire tinned with soft solder to provide high thermal resistance without electrical resistance. These segments of the electrical leads remained superconducting while carrying currents up to 0.4 ma.

Heat was applied to the calorimeter by using the joule heat developed in Formvar-covered, 0.00175-in.-diam Manganin wire, wound noninductively on the surface and held in place with General Electric 7031 varnish. (Use of this varnish as a bonding agent at low temperatures has been investigated.[3]) Manganin was used because of the small temperature coefficient of its resistivity. Power was provided by a Kintel model 301 variable dc power supply with an output of 1 to 500 volts and 0 to 20 ma. The power supply was switched into and out of the heater circuit by mercury-wetted contact relays in such a way as to keep the total resistance and the grounding of the heater circuit the same at all times. This was done to ensure that currents induced in the heater by stray laboratory fields were the same during the heating period as they were before and after, and therefore contributed a constant amount to the heat leak. The power being dissipated in the heater was determined by measuring the potential drop across the heater and across a 1000-ohm standard resistor in series with it; the measurements were made with a Leeds and Northrup type K-3 universal potentiometer. A Leeds and Northrup No. 9835-B stabilized dc microvolt amplifier was used as the null detector. The duration of a heating period was read from a Hewlett-Packard model 522B electronic counter that was triggered on and off by the appearance and disappearance of voltage in the heater circuit, counting the output signals from a

crystal-controlled oscillator. This instrument, as used here, gave the time interval of the heating period to $\pm$ 1 msec.

The temperature of the calorimeter was measured with a carbon resistance thermometer that consisted of a thin layer of Aquadag painted onto a Formex insulated copper wire located between two bare copper wires spaced about a half-inch apart. The bare wires were attached with Araldite to the Formex-insulated wire, and the latter was soldered to a strip of copper foil that was in turn attached to the calorimeter with General Electric 7013 varnish. The resistance was determined by measuring the potential drop across both the thermometer and a 10,000-ohm standard resistor in series with it. This voltage was compared with a voltage taken from a Rubicon No.2773 double six-dial thermofree potentiometer. When measuring the voltage across the thermometer, only four dials of the potentiometer were used and the unbalanced voltage was amplified with a Beckman Model 14 dc breaker amplifier and recorded on the chart of a Leeds and Northrup speedomax type G recorder. In order to reduce the joule heating in the thermometer to a negligible amount, a thermometer current between 0.1 and 1 μa was used, depending on the heat capacity of the particular calorimeter being measured. A typical carbon thermometer of this type, with a room temperature resistance of about 300 ohms, would measure 1000 ohms at 4 ^{o}K, 2000 ohms at 1 ^{o}K, and 20,000 ohms at 0.1 ^{o}K. In order to reduce the change in thermometer current with change in thermometer resistance, a 90-megohm resistor was placed in series with the thermometer. From one to four 22-1/2-v batteries were used to provide the necessary voltage.

Temperatures in the liquid helium region, 1.1 to 4.2 ^{o}K, were based

on the measurement of helium vapor pressures. The temperature scale used in the original calculations was the "T_{L55} Helium Vapor-Pressure Scale."[4] Recently, tables have become available for the "1958 He^4 Vapor-Pressure Scale of Temperatures," which has been approved by The International Committee on Weights and Measures as a standard for thermometry from 1 to 5.2 °K.[5] Hence, corrections were applied to the results of those heat-capacity runs whose accuracy was such as to justify the change. Above 2 °K, the pressure over a small amount of helium condensed in a vapor-pressure bulb was measured. The bulb has a vacuum-jacketed, thin-walled, stainless-steel tube connecting it with the manometer line at the top of the cryostat. A radiation trap consisting of four metal discs with offset holes was inserted at the lower end of the tube. Below 2 °K, the pressure over the liquid helium bath was measured at a point just below the top of the vacuum jacket of the helium Dewar. Use of the two methods was dictated by the uncertainty of corrections for hydrostatic head at temperatures above the λ-point, and thermomolecular pressure gradients existing at low temperatures. Pressures were measured with a mercury manometer down to about 30 mm of mercury. Below that they were measured with an oil manometer containing "Octoil" vacuum-pump fluid, which was about fifteen times as sensitive as the mercury manometer. The heights of the liquid columns were measured with a Wild cathetometer that could be read to ± 0.01 mm. During the vapor-pressure measurements, the helium bath was brought to the desired temperature by manipulating the valves in the line leading to a Kinney 350-cfm vacuum pump, and then the temperature of the bath was regulated to better than a millidegree by an electronic regulator of the type described by Sommers.[6] Unfortunately, the electronic regulator

did not always operate properly at temperatures above the λ-point, and so at these temperatures the bath had to be regulated by manual manipulation of a needle valve in the pumping line.

Temperatures in the adiabatic demagnetization region were based on an extrapolation of the susceptibility of copper potassium sulfate according to a Curie-Weiss law. In practice, the mutual inductance M of a set of coils surrounding the salt pill was measured with a 23-cps mutual-inductance bridge built after the design of Erickson, Roberts, and Dabbs.[7] The inductance M was related directly to the temperature by the expression $M = A + B\ (T - \Delta)^{-1}$. Constants A, B, and Δ were determined by plotting M vs $(T - \Delta)^{-1}$ for the calibration points between 1.1 and 4.2 °K. The value of Δ used in the extrapolation was that for which the best straight-line fit was obtained, 0.033 °K. The primary of the mutual-inductance coils was designed to give a uniform field over the salt pill, but a small field outside the coils. The secondary consisted of two parts, a coil at the center of the salt pill and a bucking coil below, each about one-sixth the length of the salt pill. The coil geometry, together with the small susceptibility of copper potassium sulfate, reduced to a negligible amount the effect of the nonellipsoidal shape of the salt pill on susceptibility measurements, and also minimized the nonlinearity associated with the presence of metal near the coils.

For measurements at liquid helium temperatures, it has been mentioned that the calorimeter was rigidly supported by cotton threads inside the brass cage attached to the bottom of the vapor-pressure thermometer. Thermal contact between the calorimeter and vapor-pressure thermometer was provided by a mechanical heat switch.

C. Procedures

At the beginning of a heat-capacity run, the system was cooled from room temperature to 4.2 ^{o}K without using helium exchange gas at any time. However, for samples with large lattice-heat capacity, such as the alkali metals, hydrogen-exchange gas was used down to about 14 ^{o}K, at which point the hydrogen gas was evacuated and a vacuum of about 10^{-6} mm of Hg, as measured with an untrapped ionization gauge at room temperature, was maintained in the space surrounding the calorimeter and salt pill, for the rest of the experiment. Any remaining hydrogen would freeze on the walls of the vacuum can after the system reached 4.2 ^{o}K, and hence could not spoil the vacuum. A helium-sensitive leak detector was used to check the high-vacuum system at room temperature, at liquid nitrogen temperature, at liquid helium temperature, and in the region of superfluid helium.

The mutual inductance of the coils surrounding the paramagnetic salt pill was calibrated against the vapor pressure of liquid helium at five points between 4.2 ^{o}K and 1.2 ^{o}K, with the mechanical heat switch closed. The paramagnetic salt was magnetized at 1.2 ^{o}K in a field of 7500 oersteds provided by an iron-core electromagnet. After allowing about forty-five minutes for the heat of magnetization of the 200-g salt pill to be conducted away, the mechanical heat switch was opened and the salt demagnetized. Demagnetization was accomplished slowly over a period of approximately thirty minutes, in order to reduce eddy-current heating in the calorimeter and the copper vanes embedded in the salt pill, induced by the change of the magnetic field. With the superconducting switch closed, the carbon-resistance thermometer was calibrated

against the mutual inductance of the coils surrounding the paramagnetic salt at about fifty points between 0.1 and 1.3 ^{o}K. Since heat was leaking into the system at about 100 ergs/min, the calibration was made by taking simultaneous readings of mutual inductance and thermometer voltage, at temperature intervals ranging between 0.05 and 0.09 T. After reaching 0.2 ^{o}K, the temperature of the salt pill was raised between successive calibration points by supplying power to a heater attached to the copper shield. About two minutes were required to obtain thermal equilibrium between the salt pill and the carbon thermometer following each heat input at that temperature, but slightly less time was needed as the temperature increased. Below 0.2 ^{o}K it took longer to obtain thermal equilibrium, and so the system was allowed to warm up at its natural rate.

The temperature T was represented as a function of the resistance R to within 1% by $T^{-1} = C_0 + C_1 R + C_2 R^2 + C_3 R^3 + C_4 R^4$. Constants C_0, C_1, C_2, C_3, and C_4 were computed by a least-squares program on a digital computer. The computer program was set up to calculate temperatures from this equation for the resistances measured during the heat capacity. Also, for each calibration point, it calculated the fractional deviation between the observed temperature and the temperature calculated from the equation. A smooth curve drawn through these fractional deviations plotted against calculated temperature was used to ascertain the true temperatures from those calculated from the equation.

Following a second demagnetization, the superconducting switch was opened to leave the calorimeter thermally isolated from the salt pill, and heat-capacity measurements were made. Before the salt pill

warmed up appreciably, it was possible to make several series of measurements covering a range of a few tenths of a degree, and this was done. The calorimeter was returned to its original temperature at the end of each series by closing the superconducting switch. When measurements in that temperature range were complete, the temperature of the salt pill was increased by supplying power to the heater attached to the copper shield. The process was repeated covering each range up to 1.3 ^{o}K at least twice.

The quantity of heat introduced is known from measurements of the length of the heating period and the heater power. Typical heating curves are shown in Fig. 2. Temperature increments of from 1/15 to 1/10 of the absolute temperature were calculated by extrapolating the initial and final temperature drifts to the middle of the heating period. Heater power was selected so that the heating periods were usually between 10 and 40 secs. The gain of the amplifier was set so that the change in thermometer voltage due to the heat input was equivalent to two or more chart widths on the recording potentiometer.

Measurements at liquid helium temperatures were made with the mechanical heat switch providing thermal contact between the calorimeter and the vapor pressure bulb. The carbon-resistance thermometer was calibrated against the vapor pressure of liquid helium at twenty points between 1.1 and 4.2 ^{o}K. In this region, the temperature T was represented as a function of the resistance R to within 1/2 of 1% by $T^{-1} = C_0 \log^{-1} R + C_1 + C_2 \log R + C_3 \log^2 R + C_4 \log^3 R$. The heat-capacity measurements and their calculation was carried out in the same way as described for the adiabatic demagnetization region.

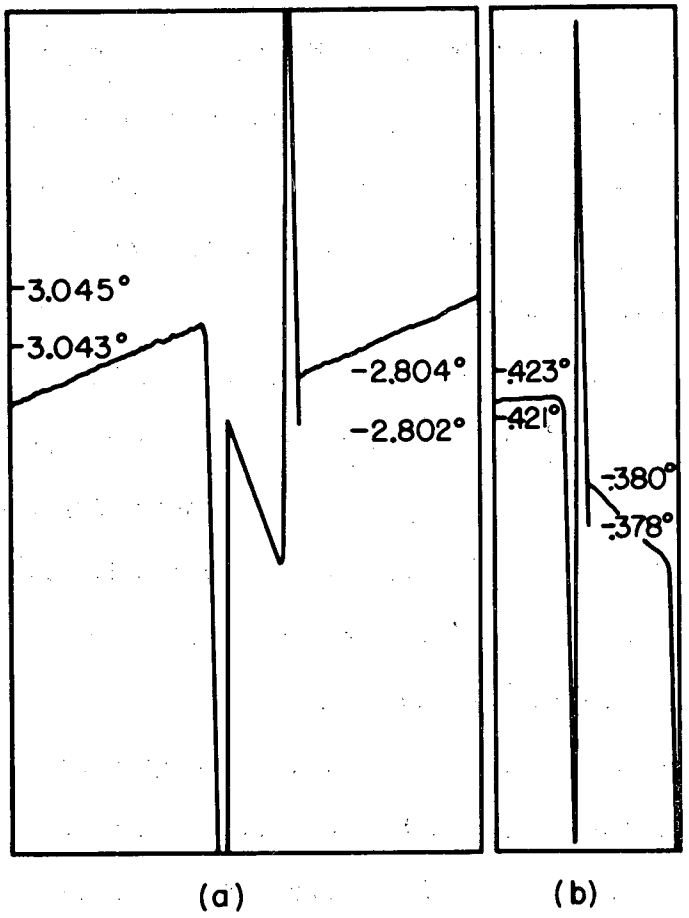

MU-25022

Fig. 2. Typical heating curves: (a) Heat capacity point in the liquid helium region. The abrupt outer changes in slope occur at the beginning and end of the heating period; the others are produced by changing the amplifier gain or potentiometer voltage. (b) Heat capacity point in the adiabatic demagnetization region.

II. HEAT CAPACITY OF SODIUM, POTASSIUM, RUBIDIUM, AND CESIUM

A. Introduction

The alkali metals are ideal examples for theoretical treatment of electronic structure because they have a single valence electron and their nearest neighbor distance is large compared with their ionic radius. The only other monovalent metals, copper, silver, and gold, are complicated by the fact that their outer-most filled electronic shell is a d-shell that is more spread out than the p-shell of the alkali metals and thus has a greater effect on the outer s-electron. There have been a large number of theoretical investigations of the electronic band structure of the alkali metals, and consequently, experimental determination of their properties, specifically the electronic heat capacity, is of considerable interest. This quantity would provide a comparison with the predicted effects of electron-electron and electron-phonon interactions. In addition, the lattice heat capacity would provide a test of the lattice dynamic calculations that have been made for the cubic metals, but which have not yet been subjected to experimental verification.

So far, very little experimental work has been done. Owing to their chemical properties, the alkali metals are somewhat more difficult to handle than most other metals, and it is only recently that sufficiently large quantities of rubidium and cesium have become available in a state pure enough to make measurements on them worthwhile. As will be shown below, measurements on potassium, rubidium, and cesium must be made below 1 ^{o}K to obtain their electronic heat capacity. In this temperature range, calorimetric techniques have only recently been developed.

In lithium and sodium the experimental situation is complicated by the existence of a martensitic phase transformation found by Barrett.[8] The transformation sets in at about 80 ^{o}K for lithium, and at about 36 ^{o}K for sodium. In both metals, the high-temperature body-centered cubic phase is partially transformed to the hexagonal close-packed phase to an extent determined by the thermal and mechanical history of the particular specimen. Roberts has measured the heat capacities of lithium and sodium from 1.5 to 20 ^{o}K.[9] However, Rayne, making measurements on sodium below 1 ^{o}K, observed an anomaly in its heat capacity at about 0.9 ^{o}K which he associated with the martensitic transformation, although the connection seems rather doubtful in view of what is known about this type of transformation.[10]

The present work includes measurements on sodium from 0.15 to 1.4 ^{o}K, and on potassium, rubidium, and cesium from 0.15 to 4.2 ^{o}K. The sodium measurements were made to investigate the reported anomaly, and the other measurements for a comparison with theories of the lattice and electronic heat capacities.

At low temperatures, the heat capacity C of a normal metal is generally considered to be the sum of an electronic and a lattice heat capacity, C_L:

$$C = \gamma T + C_L$$
$$C_L = AT^3 + BT^5 \ . \ . \ . \qquad (2)$$

In this expression, A and B are constants characteristic of the lattice, T is the temperature, and γT is the electronic heat capacity with γ given by

$$\gamma = \frac{1}{3} \pi^2 k^2 N (E_F), \qquad (3)$$

where k is Boltzmann's constant, and $N(E_F)$ is the number of energy states per unit energy range per mole at the Fermi energy E_F. This result was first obtained by Sommerfeld.[11] Bloch has shown that Eq. (3) is valid, and independent of the condition of binding of the electronic system.[12] For a free electronic system, such as might be assumed to be approximately represented by the s-electrons in the monovalent metals, $N(E_F)$ is given by

$$N(E_F) = \frac{2\pi mV}{h^2} \left(\frac{3n}{\pi}\right)^{1/3}, \tag{4}$$

where m is the free electron mass, n the number of electrons per cm^3, V the molar volume of the metal, and h is Planck's constant. For free electrons, then:[11]

$$\gamma = \frac{4\pi^3 mk^2 V}{3\,h^2} \left(\frac{3n}{\pi}\right)^{1/3} = 1.360 \times 10^{-4}\, V^{2/3}\, n_a^{1/3}\ \frac{\text{joules}}{\text{mole-deg}^2}, \tag{5}$$

where n_a is the number of valence electrons per atom.

Although the free-electron model gives closer agreement to experimentally determined values of γ than one would guess from the simple assumptions made by the theory, it is not exact, and so more refined calculations of $N(E_F)$ must be made. It is customary to keep the form of Eq. (5), and of other expressions based on the free electron model, by replacing the electron mass m with an effective electron mass m^*. Kittel gives a natural definition of the effective mass as being the mass a free electron would need in order for the velocity increment under an applied impulse to be equal to the actual velocity increment of the conduction electron under the same impulse.[13] Effective masses defined in terms of different properties of a metal may differ from each other depending on details of the band structure. The ratio m_t^*/m, where m_t^*

is the "thermal effective mass," is defined by γ (experimental)/γ (free electron).

Band-theory calculations on the alkali metals, giving the effect of the periodic potential of the ion cores situated at the lattice sites on the effective mass ratio, have been carried out by Brooks.[14] Cohen and Heine have developed a simple, semiquantitative scheme for the band structure which embraces all the monovalent metals and serves as a basis for comparison with experiment.[15] Pines has investigated the effect of electron-electron interactions[16] and Buckingham and Schafroth have investigated electron-phonon interactions.[17]

Within the low-temperature limit, the lattice heat capacity is given by the elastic continuum model of Debye, from which the T^3 term in Eq. (2) is derived.[18] The Debye characteristic temperature at the absolute zero, Θ_0, and the coefficient A of the T^3 term, are related by $A = 12/5\ \pi^4\ R\ \Theta_0^{-3}$, and are determined completely by the elastic constants. In the original Debye theory, only the T^3 term was important up to $\Theta_0/12$. However, Blackman points out that for real crystals one must have $T < \Theta_0/50$ or even $T < \Theta_0/100$ before the T^3 region is sure.[19,20] If a plot of C/T vs T^2 approaches a straight line in this range of temperatures, the intercept determines γ directly, and Θ_0 can be calculated from its slope. The T^5 term in C_L has been calculated by de Launay for the cubic metals, on the basis of a model employing central force interactions between first and second neighbors and treating the conduction electrons as a free-electron gas.[21] The force constants are evaluated from the elastic constants, and the theory gives B in terms of the elastic constants.

B. Results

Under an argon atmosphere, each sample was cast into a calorimeter which was then sealed. The design of the calorimeter used for potassium, rubidium, and cesium is shown in Fig. 3. Each part was machined from a single piece of copper. Before the alkali metal solidified, the cap was inserted and sealed to the body of the calorimeter with Woods metal. This design was chosen to ensure good thermal contact between the alkali metal and the calorimeter, and to prevent contact of the alkali metal with any solder.

The heat capacity of one empty calorimeter was measured from 1.1 to 4 ^{o}K and was found to be in reasonable agreement with that estimated from the heat capacities of its constituents: copper,[22-25] Woods metal,[26] General Electric 7031 varnish,[27] and Manganin.[25] Corrections for the slightly different amounts of the various materials in the other calorimeters were estimated from their known heat capacities, and amounted to no more than 2% of the heat capacity of the filled calorimeter. Most of this correction was for the different amounts of copper, for which the heat capacity is known to within 1%. The calorimeter used for sodium was appreciably different in design, but it also was almost entirely copper, so that the uncertainty in its heat capacity was not serious. Below 2°K, the heat capacity of the empty could be represented by the sum of two terms, one linear and one cubic in temperature. Above 2 ^{o}K, graphic means were used to subtract off the contribution of the empty.

It should be mentioned here that the first two attempts to measure the heat capacity of an empty calorimeter between 1.1 and 4 ^{o}K led to unexpectedly high results. Below 3 ^{o}K, the heat capacity was 40% to 80%

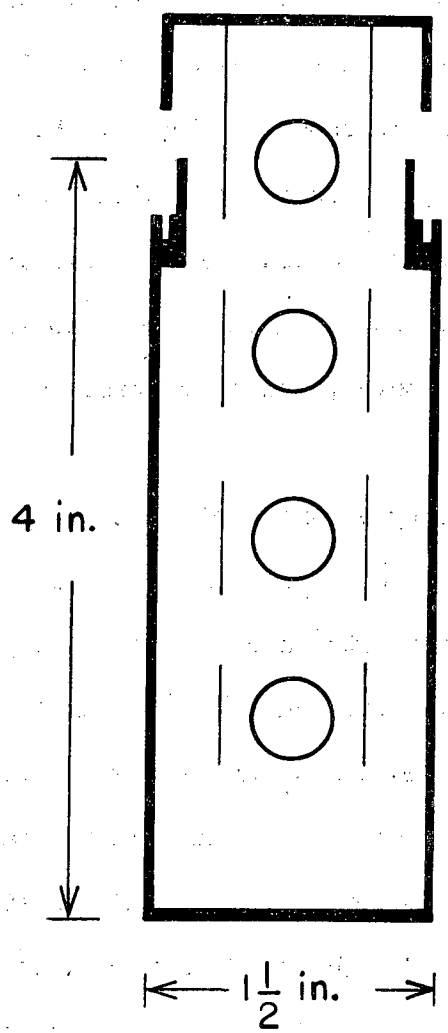

MU-25008

Fig. 3. Schematic drawing of the calorimeter used for potassium, rubidium, and cesium.

higher than estimated. Investigation showed that this was due to the presence of approximately 0.1 g of air sealed into the calorimeter. After the second of these runs, the calorimeter seal was cracked to permit escape of the air when the space surrounding the calorimeter was evacuated, and the measurement was repeated without otherwise changing the apparatus. The heat capacity was then found to be close to that estimated for the calorimeter. Thus, the difference between the last two runs gives the heat capacity of solid air which is reported and briefly discussed in the Appendix.

The 62.445-g sample of sodium was obtained from Baker and Adamson and was labelled reagent grade. The 76.367-g sample of potassium, obtained from United Mineral and Chemical Corporation was also labelled reagent grade. The 125.847-g rubidium sample and the 113.080-g cesium sample were also obtained from United Mineral and Chemical Corporation and both were stated to be 99.8% pure. These samples were of the highest commercially available purity. All sample weights were corrected for buoyancy.

The first cesium obtained from United Mineral and Chemical Corporation, which came sealed in glass ampules, was observed to be completely liquid at room temperature even though the melting point of pure cesium is 28.5 °C. It did not completely solidify until cooled to about 12 °C. More cesium obtained from the same company proved to be about 90% in the solid phase at 25 °C. It was from this second lot that the cesium sample was taken. (Another sample obtained from A.D. MacKay of 99.9% stated purity acted similarly.) The depression in the freezing point of the cesium indicated that it was less than 99.8% pure, and so a spectroscopic analysis was made. A spectroscopic analysis was also made on the

potassium and rubidium used. The only impurities of any consequence in each case turned out to be other alkali metals. This was fortunate, as the electronic properties of an alkali metal would be much less affected by small amounts of other alkali metals than by similar amounts of polyvalent metals.

The results of the spectroscopic analysis were: the cesium sample contained 0.2% Na, 0.2% K, and 0.4% Rb; the potassium sample contained 0.5% Na; and the rubidium sample contained 6% K and 0.1% Cs. This analysis gives the amount of impurity to within a factor of two. Since the rubidium sample contained so much potassium, a chemical analysis was run on it. A sample of rubidium was converted to the chloride, weighed, and analyzed for total amount of chloride ion present. This information, along with the assumption that potassium was the only impurity present, made it possible to calculate the amount of potassium present in the rubidium sample (it was 3%).

The heat-capacity measurements below 1 $^{\circ}$K were at first calculated on the basis of a temperature scale obtained by extrapolation of the susceptibility of copper potassium sulfate from above 1 $^{\circ}$K according to a Curie-Weiss law, in the manner described previously in Sec. I. This temperature scale was originally chosen because thermodynamic measurements suggested that it was a good approximation to the absolute temperature.[28] However, measurements based on this temperature scale on copper,[25] gallium,[25] aluminum,[27] and zinc,[29] for which the heat capacity can be assumed known, have led to results that are too high at temperatures below 0.3 $^{\circ}$K. Phillips has calculated a correction to the temperature scale from his heat capacity measurements[30] and the result suggests that the susceptibility-temperature relation of Cooke, Meyer, and Wolf[31]

is more nearly correct that a Curie-Weiss law. This correction has been applied to the potassium, rubidium, and cesium measurements, but not to the sodium measurements, as the data above 0.3 ^{o}K were sufficient to determine the results of interest for sodium.

The experimental data for potassium, rubidium, and cesium between 0.15 and 4.2 ^{o}K are collected in Tables I-VI, and the points obtained below 1.2 ^{o}K are shown as plots of C/T vs T^2 in Figs. 4, 5, and 6. Sodium is plotted in Fig. 7. Even after the application of the temperature scale correction, the lowest points for potassium, rubidium, and cesium show positive deviations from a straight line of 3% to 6%. In view of the experience with the temperature scale referred to above, it seems unlikely that such large errors at 0.15 ^{o}K would be produced by errors in the temperature scale. It appears reasonable to suppose that the additional heat-capacity contribution is produced by the interaction of the nuclear quadrupole moment with electric field gradients in the neighborhood of impurity atoms or physical defects. The relatively high impurity content, strains produced on cooling, and the high values of the Sternheimer antishielding factor, could account for the difference in behavior between these samples and the other metals on which measurements have been made.

The points obtained in the adiabatic demagnetization region do not join smoothly the points obtained at liquid helium temperatures. For potassium and cesium there is a difference of 1.5% and 3% respectively. In each case, the points obtained in the adiabatic demagnetization region are higher. This effect has not been observed in other experiments in the same apparatus. It is believed that this is a result of a superheating of the copper calorimeter during the heating period,

Table I. Heat capacities of potassium in the adiabatic demagnetization region. Values are in millijoules $mole^{-1}$ deg^{-1}.

T	C	T	C	T	C
0.1635	0.3641	0.3985	1.009	0.4798	1.295
0.1818	0.4058	0.4266	1.108	0.5254	1.475
0.2018	0.4489	0.4571	1.212	0.5656	1.658
0.2206	0.4949	0.2022	0.4495	0.6118	1.884
0.2387	0.5403	0.2234	0.4993	0.6611	2.145
0.2577	0.5900	0.2422	0.5455	0.7153	2.454
0.2757	0.6352	0.2624	0.6018	0.7695	2.803
0.2933	0.6828	0.2864	0.6623	0.8296	3.231
0.1579	0.3538	0.3101	0.7264	0.8921	3.766
0.1737	0.3888	0.3365	0.8004	0.7234	2.507
0.1928	0.4315	0.3633	0.8872	0.7783	2.883
0.2121	0.4761	0.3926	0.9775	0.8332	3.298
0.2293	0.5191	0.4223	1.078	0.8901	3.759
0.2471	0.5645	0.4507	1.181	0.8710	3.596
0.2673	0.6179	0.4828	1.305	0.9334	4.110
0.2873	0.6697	0.4963	1.356	1.0128	4.894
0.3049	0.7150	0.5429	1.554	1.1005	5.884
0.3254	0.7744	0.5940	1.787	1.1802	6.881
0.3465	0.8387	0.6411	2.029	1.2180	7.397
0.3723	0.9192	0.6898	2.301	1.2378	7.707

Table II. Heat Capacities of potassium in the liquid helium region. Values are in millijoules $mole^{-1}$ deg^{-1}.

T	C	T	C
1.1606	6.519	1.1421	6.278
1.2392	7.585	1.2033	7.115
1.3243	8.898	1.2834	8.269
1.4162	10.49	1.3918	10.07
1.5274	12.75	1.4897	11.97
1.6458	15.50	1.5884	14.12
1.7582	18.40	1.6968	16.80
1.8741	21.90	1.8162	20.15
1.9978	26.14	1.9358	24.00
2.1300	31.36	2.0585	28.47
2.2725	37.81	2.1932	34.11
2.4205	45.44	2.3415	41.30
2.5738	54.67	2.5007	50.26
2.7357	65.88	2.6600	60.48
2.9140	79.98	2.8279	73.27
3.1103	98.09	3.0084	88.62
3.3140	119.9	3.2078	108.6
3.5308	146.4	3.4143	132.1
3.7669	179.5	3.6325	160.6
4.0309	223.1	3.8819	198.1
		4.1012	236.2

Table III. Heat capacities of rubidium in the adiabatic demagnetization region. Values are in millijoules $mole^{-1}$ deg^{-1}.

T	C	T	C	T	C
0.1569	0.4546	0.1795	0.5277	0.4992	2.686
0.1753	0.5093	0.2038	0.6137	0.5384	3.154
0.1948	0.5787	0.2288	0.7091	0.5859	3.807
0.2148	0.6513	0.2517	0.8077	0.6411	4.681
0.2356	0.7350	0.2773	0.9295	0.7047	4.872
0.2587	0.8392	0.3028	1.067	0.7731	7.394
0.2914	0.9999	0.3267	1.206	0.8493	9.397
0.1506	0.4351	0.3495	1.356	0.9285	11.88
0.1695	0.4948	0.3817	1.587	1.0110	14.95
0.1897	0.5626	0.4166	1.870	1.0984	18.84
0.2097	0.6300	0.4516	2.189	0.6374	4.614
0.2283	0.7040	0.4872	2.545	0.7078	5.945
0.2517	0.8064	0.5242	2.981	0.7857	7.727
0.2794	0.9398	0.5677	3.552	0.8630	9.829
0.3121	1.118	0.6144	4.226	0.9451	12.50
0.3440	1.314	0.6566	4.930	1.0409	16.27
0.3802	1.573	0.7239	6.263	1.1354	20.69
0.4173	1.874	0.7964	7.943	1.2367	26.40
0.4604	2.266	0.8704	10.01	1.2144	25.10
0.5005	2.696	0.4156	1.866	1.1670	22.43
0.5539	3.352	0.4585	2.264	1.2457	26.83

Table IV. Heat capacities of rubidium in the liquid helium region. Values are in millijoules $mole^{-1}$ deg^{-1}.

T	C	T	C
1.1991	24.07	1.9314	104.3
1.3249	32.22	2.1287	142.6
1.4630	43.46	2.3342	191.4
1.6163	59.22	2.5471	251.8
1.7867	81.31	2.7886	336.9
1.9718	111.4	3.0530	445.1
2.1610	149.7	3.3361	581.4
2.3660	200.3	3.6579	757.7
2.5961	269.1	4.0081	969.1
2.8521	361.7	1.5881	55.89
3.1428	486.5	1.7361	73.97
3.4535	644.5	1.9055	99.58
3.7762	827.6	2.0910	134.4
4.0713	1009.	2.2887	179.3
1.1952	23.83	2.5015	238.5
1.3076	30.99	2.7254	313.0
1.4365	41.12	2.9798	412.5
1.5882	56.00	3.2642	543.7
1.7523	76.35	3.5784	711.6
		3.9231	914.7

Table V. Heat capacities of cesium in the adiabatic demagnetization region. Values are in millijoules mole^{-1} deg.$^{-1}$.

T	C	T	C	T	C
0.1634	0.7338	0.5590	7.502	0.7447	16.17
0.1807	0.8326	0.6036	9.172	0.8051	20.24
0.2018	0.9667	0.6527	11.28	0.8786	26.06
0.2308	1.175	0.7109	14.22	0.9505	32.95
0.2532	1.372	0.2026	0.9720	1.0318	41.97
0.2801	1.643	0.2177	1.079	1.1158	53.33
0.3116	2.001	0.2319	1.193	1.2150	69.78
0.1517	0.6690	0.2482	1.329	1.1431	57.95
0.1677	0.7574	0.2706	1.542	1.2360	73.57
0.1858	0.8665	0.2955	1.802	0.5271	6.482
0.2089	1.023	0.3127	2.010	0.5778	8.172
0.2375	1.239	0.3313	2.258	0.6298	10.27
0.2594	1.440	0.3575	2.640	0.6862	12.91
0.2853	1.709	0.3895	3.172	0.7482	16.41
0.3140	2.043	0.4168	3.713	0.8116	20.63
0.3410	2.401	0.4519	4.458	0.8438	23.09
0.3696	2.845	0.4942	5.520	0.9162	29.45
0.4035	3.447	0.5458	7.064	1.0005	38.41
0.4349	4.074	0.5930	8.747	1.0967	50.96
0.4734	4.992	0.6439	10.87	1.1986	66.93
0.5192	6.242	0.6929	13.29		

Table VI. Heat capacities of cesium in the liquid helium region. Values are in millijoules $mole^{-1}$ deg^{-1}.

T	C	T	C
1.2031	65.61	1.1779	61.56
1.2932	82.03	1.2459	73.14
1.3883	102.8	1.3371	91.29
1.4897	128.8	1.4374	114.7
1.6006	161.6	1.5444	144.1
1.7185	202.8	1.6575	180.2
1.8435	253.2	1.7799	226.0
1.9803	317.3	1.9111	282.1
2.1302	397.5	2.0522	351.8
2.2875	492.0	2.2053	439.2
2.4529	605.4	2.3645	541.2
2.6285	735.7	2.5355	662.7
2.8182	892.4	2.7183	805.4
3.0238	1077.	2.9183	978.2
3.2512	1299.	3.1364	1185.
3.5012	1566.	3.3691	1421.
3.7667	1861.	3.6290	1702.
4.0437	2180.	3.8761	1978.
		4.0880	2217.

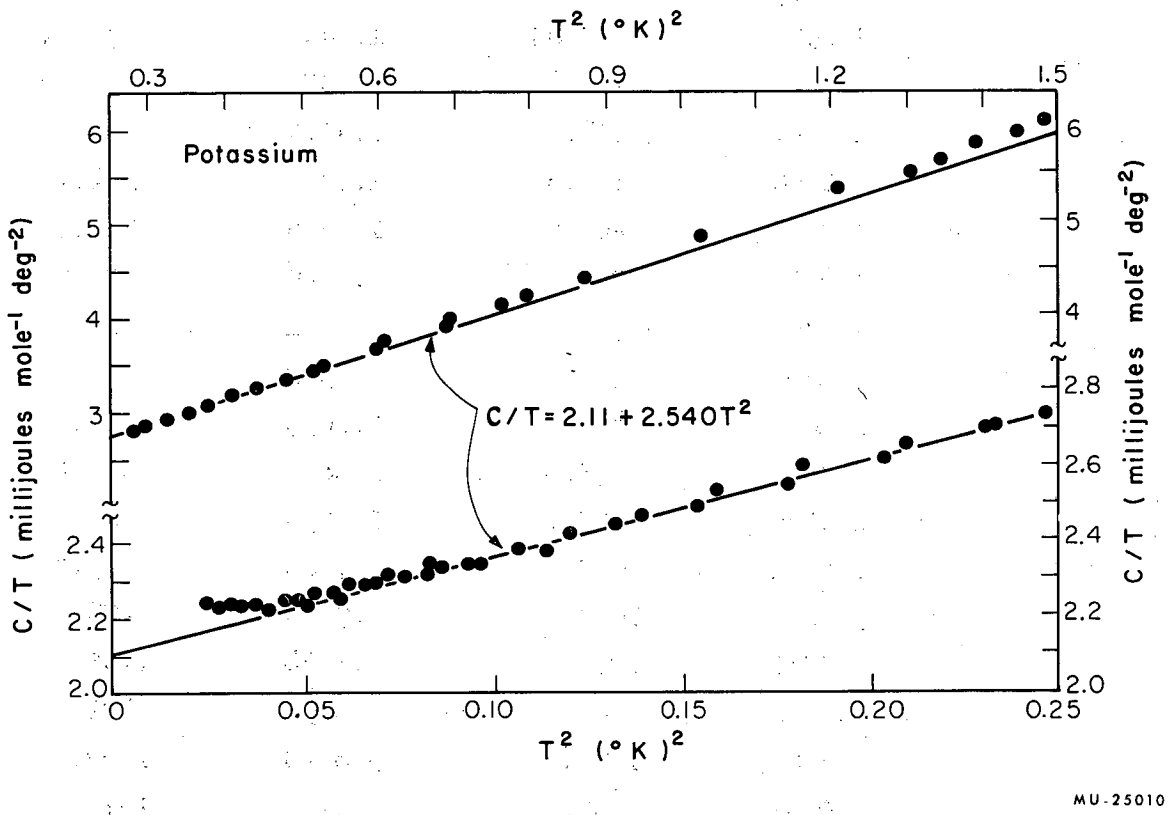

Fig. 4. C/T vs T^2 for potassium. Circles represent points in the adiabatic demagnetization region. Squares represent points in the liquid helium region.

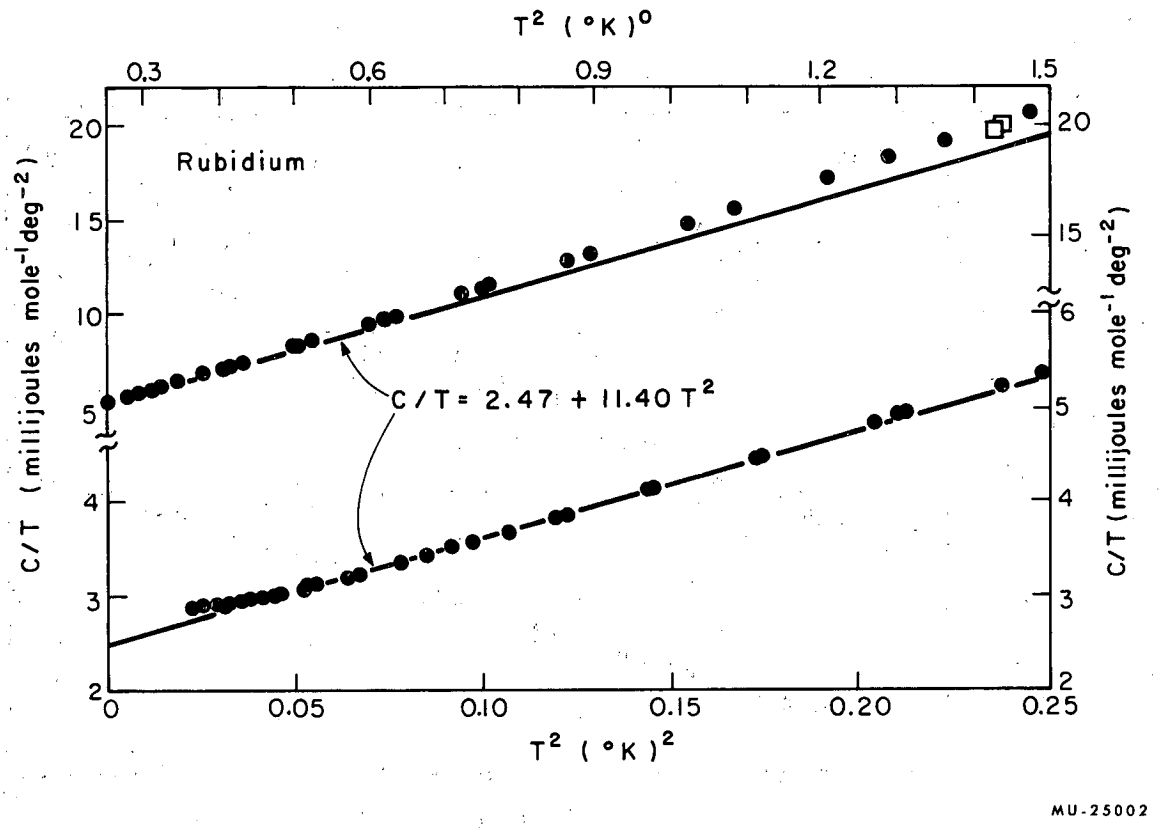

Fig. 5. C/T vs T^2 for rubidium. Circles represent points in the adiabatic demagnetization region. Squares represent points in the liquid helium region.

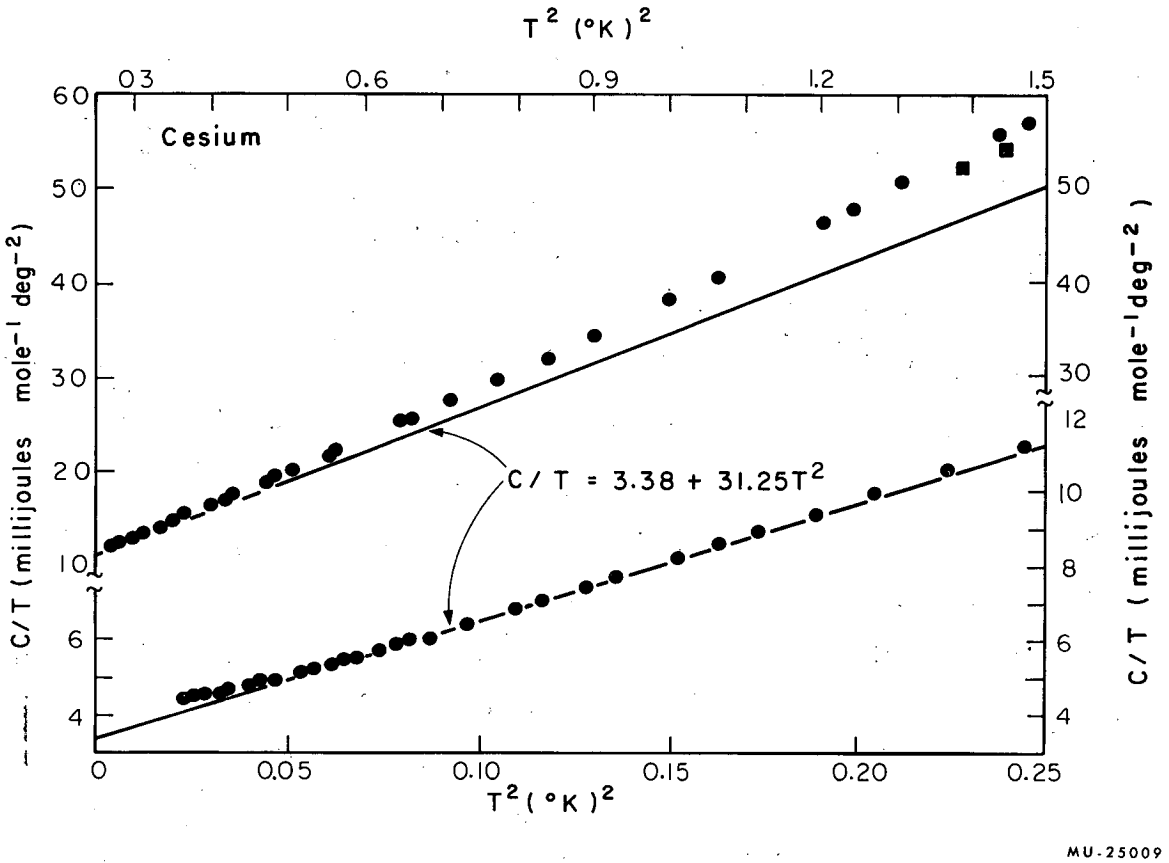

Fig. 6. C/T vs T^2 for cesium. Circles represent points in the adiabatic demagnetization region. Squares represent points in the liquid helium region.

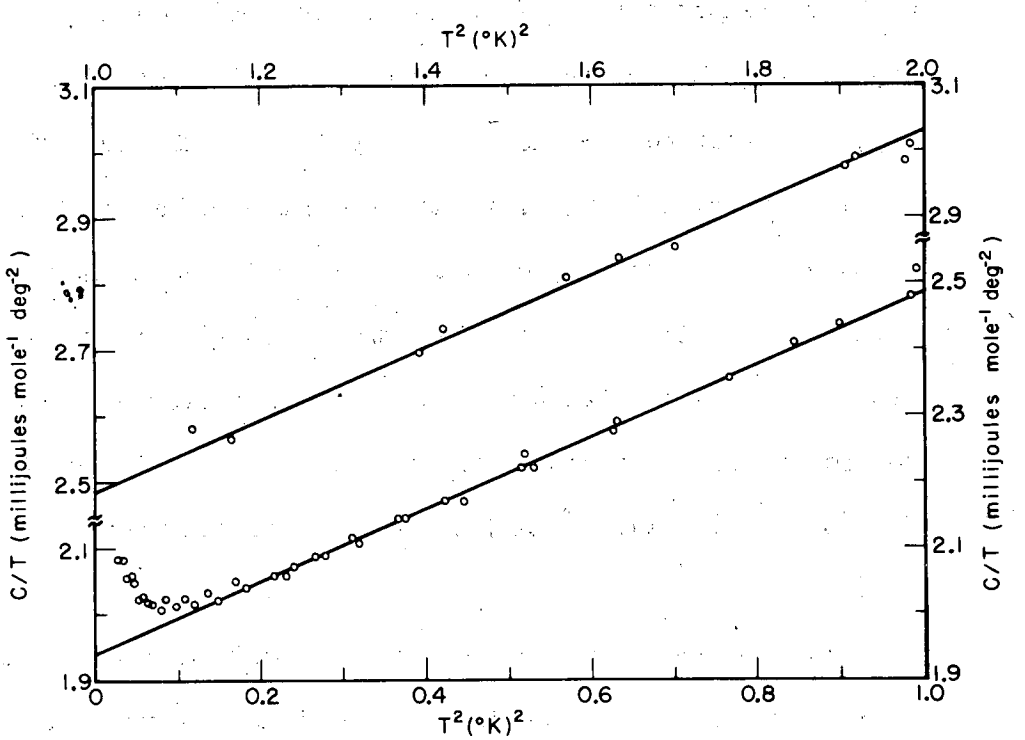

Fig. 7. C/T vs T^2 for sodium. C is the heat capacity of sample plus calorimeter per mole of sample. The equation for the straight line is $C/T = 1.94 + 0.544\ T^2$. The correction to C/T for the calorimeter was estimated from the known heat capacities of the material used (largely copper), and is $0.50 + 0.037\ T^2$ millijoules $mole^{-1}\ deg^{-2}$. Thus, for sodium, $C/T = 1.44 + 0.507\ T^2$ millijoules $mole^{-1}\ deg^{-2}$.

which produces a larger flow of heat to the surroundings than during the drift periods, with a consequent overestimate of the energy increment of the sample. This effect would be largest at the higher temperatures in the adiabatic demagnetization region, where the thermal resistance of the superconducting switch is low and the heating power is higher than at lower temperatures. It would not be important in the liquid helium region where the calorimeter is always well isolated from its surroundings and their heat exchange is negligible. The fact that the effect was larger in the potassium and cesium measurements than in the rubidium measurements correlates with the observation that the superconducting switch had a higher thermal resistance in the latter experiment. In other experiments with this apparatus the heater was attached directly to the sample, eliminating the possibility of a direct flow of heat from the heater and through the superconducting switch to the surroundings.

For the above reasons, we believe that the most reliable heat-capacity points are those in the liquid helium region and those between 0.3 and approx 0.7 $^{\circ}$K. This view is supported by the observation that the points in those two regions fit a single smooth curve, though plotted in several different ways.

The values of γ and A in Eq. (2) are usually obtained either from the limiting slope of a graph of C/T vs T^2, or by a least-squares fit of C to a power series in T containing the first, third, and possibly fifth powers. Neither of these methods is appropriate in the present case. The lowest points obviously include a heat-capacity contribution not included in Eq. (2). Some of the intermediate points should be given less weight, and the points at the highest temperatures are outside

the range of validity of any simple expression for the lattice heat capacity. The method actually used in obtaining these parameters was as follows. Preliminary values of γ were obtained from the plots of C/T vs T^2. For sodium and potassium, γ was determined unambiguously by this method; for rubidium, and particularly for cesium, the temperature range over which a straight-line fit was assumed was somewhat arbitrary. The resulting γ values, together with values differing by 1% and 2% in each direction, were then used to construct a series of plots of $(C - \gamma T)/T^3$ vs T^2. The resulting curves should be linear to higher temperatures than the plots of C/T vs T^2. According to Blackman's calculations, the straight-line region might be expected to extend to $T = \theta_0/30$.[19] The γ values finally adopted were those for which this latter plot approximated a straight line over the widest range of temperatures.

The resulting plots are shown for potassium, rubidium, and cesium in Figs. 8,9, and 10, and are in fact linear up to $T \approx \theta_0/30$. Changes in γ of $\pm$ 1% from the values used in these plots produced conspicuous curvature in the neighborhood of $\theta_0/100$. A and B, the coefficients of the T^3 and T^5 terms of the lattice heat capacity, were respectively determined from the intercept and slope of these plots. Values of A, B, and γ are given in Table VII.

On the basis of past experience with the apparatus, the precision expected is a few tenths of a percent at liquid helium temperature, and about 1% in the adiabatic demagnetization region. These figures also apply to the present measurements with the one exception noted above. The accuracy, difficult to estimate, is almost certainly determined by errors in temperature measurement, including possible errors in the

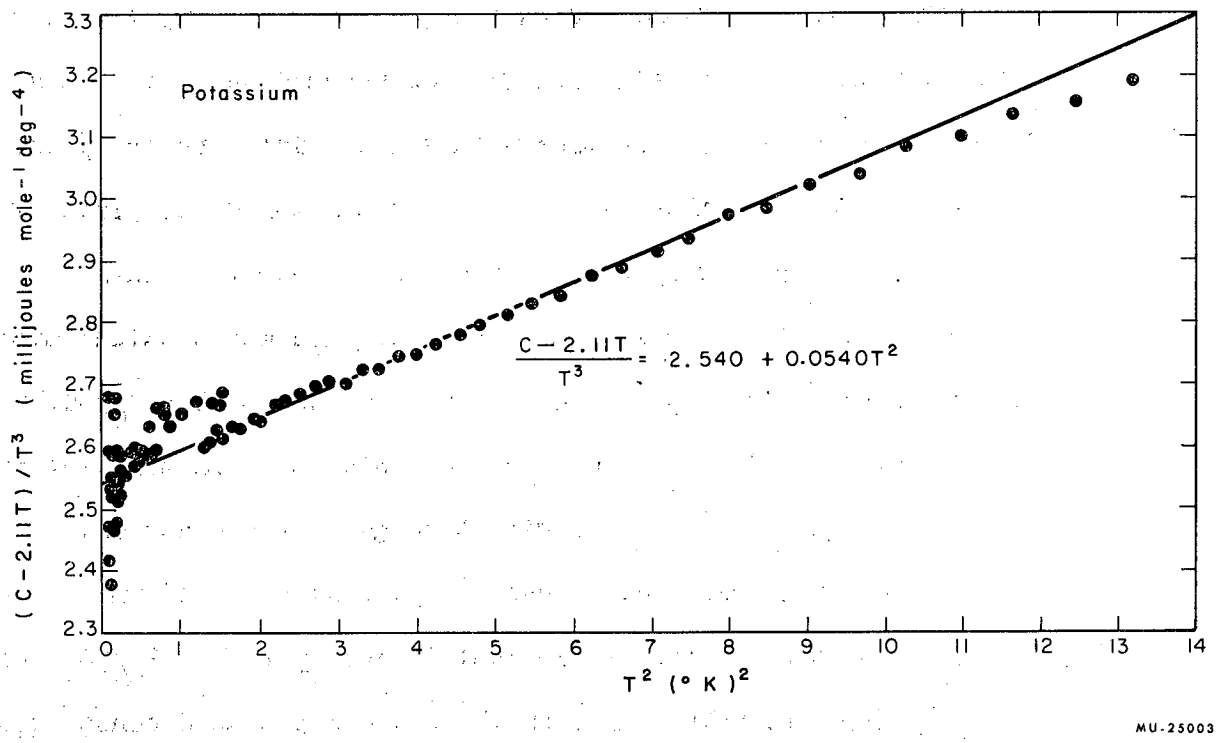

Fig. 8. $(C-2.11\ T)/T^3$ vs T^2 for potassium.

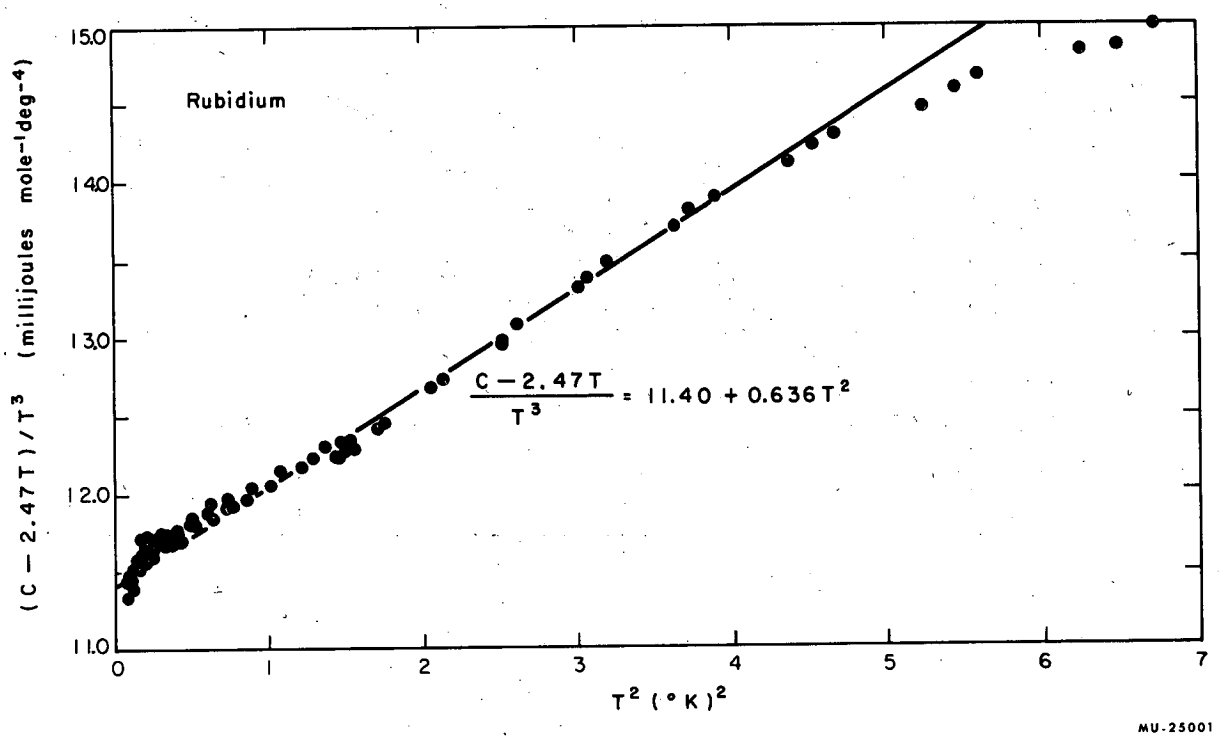

Fig. 9. $(C-2.47\ T)/T^3$ vs T^2 for rubidium.

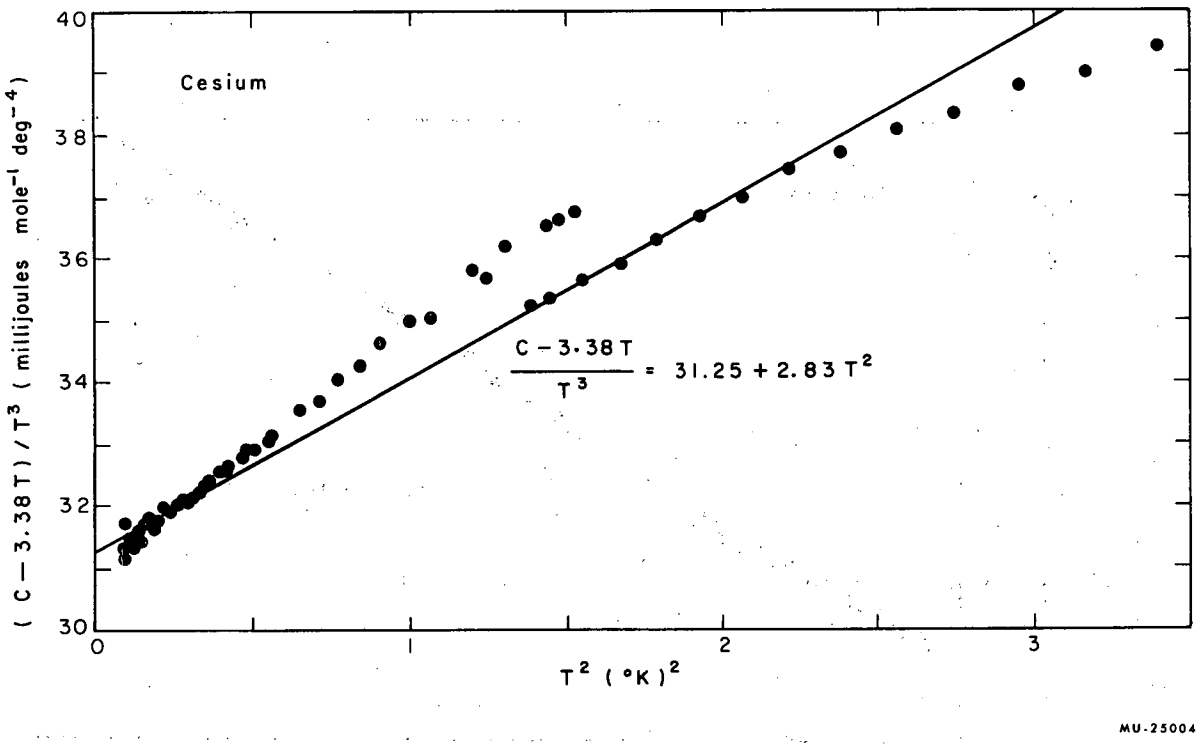

Fig. 10. $(C-3.38\ T)/T^3$ vs T^2 for cesium.

Table VII. The coefficient of the first, third, and fifth power of temperature describing the heat capacities up to $T \approx \theta_0/30$, where $C = \gamma T + AT^3 + BT^5$.

	Na	K	Rb	Cs
γ (millijoules mole^{-1} deg^{-2})	$1.44 {}^{+0}_{-0.03}$	2.11 ± 0.02	2.47 ± 0.05	3.38 ± 0.07
A (millijoules mole^{-1} deg^{-4})	0.507 ± 0.015	2.540 ± 0.025	11.40 ± 0.10	31.25 ± 0.20
B (millijoules mole^{-1} deg^{-6})	-	0.0540 ± 0.0020	0.636 ± 0.020	2.83 ± 0.10

helium vapor-pressure scale, the vapor-pressure measurement, and the extrapolation to below 1 ^{o}K. The resulting error seems likely to be no more than 0.5% at liquid helium temperatures, 1% down to 0.25 ^{o}K, and 2 or 3% at 0.15 ^{o}K. The limits of error indicated in Table VII represent qualitative estimates based on these figures and take into account the method of analysis of the data.

For sodium, the data were not recalculated on the corrected temperature scale; the γ value quoted is therefore likely to be approximately 1% high. The measurements on sodium are in good agreement with those of Martin,[32] who found no significant change in either γ or A for samples with different amounts of the hexagonal close-packed phase.

For potassium, rubidium, and cesium, there is no reason to expect the heat capacity to depend on sample treatment,[8] and the results are compared with other experimental data in the liquid helium region in Table VIII. Since most of the other work does not go to low enough temperatures to permit an analysis of electronic and lattice heat capacities, comparison is made on the basis of total heat capacity. The potassium measurements agree well with those of Roberts, except at 1.5 ^{o}K, where Roberts' values include a correction for effects of helium-exchange gas which could very well account for the discrepancy. In some cases the disagreement with the other measurements on rubidium and cesium may exceed the combined experimental errors, suggesting that the result is affected by sample purity. Neither McCollum[33] nor Manchester[34] give analyses of their samples, but these were obtained commercially and are unlikely to be appreciably purer than those used in the present measurements.

Table VIII. Comparison of experimental data with other work in the liquid helium region.

Metal	C (millijoules mole^{-1} deg^{-1})				Reference
	1.5 °K	2.0 °K	3.0 °K	4.0 °K	
K	12.2	26.3	87.8	218	This work
K	12.7	26.4	86.6	215	L.M. Roberts
Rb	47	117	423	963	This work
Rb	48	120	440	972	D.C. McCollum
Rb	46	107	391	898	F.D. Manchester
Cs	131	326	1054	2124	This work
Cs	129	310	990	1980	D.C. McCollum

[a] See Ref. 9

[b] See Ref. 33

[c] See Ref. 43

C. Discussion

1. Sodium

Sodium is distinguished from the other alkali metals studied in that it undergoes a martensitic phase transformation on cooling. At 36 ^{o}K a hexagonal close-packed phase with atomic volume equal to that of the body-centered cubic phase appears and increases to 25% to 50% of the total at low temperatures, the amount depending on sample history. Barrett has shown that the amount transformed approaches a constant value at low temperatures and in particular that no further transformation occurs at liquid helium temperatures.[8] This behavior is typical of martensitic transformations in general and makes it seem unlikely that the anomaly reported by Rayne at 0.9 ^{o}K could have been associated with the transformation. The present experiments show no sign of an anomaly between 0.15 and 1.4 ^{o}K. It seems most probable that Rayne's anomalous results were connected with the use of helium-exchange gas, although the possibility that it is due to a difference in sample history or purity is not excluded.

The values of γ and θ_o calculated from the heat-capacity data are 1.44 millijoules mole^{-1} deg^{-2} and 156.5 ^{o}K. These figures of course represent an average for the two phases present, but the experiments of Martin[32] suggest that they are approximately the same for the two phases. Therefore they may be taken as rough values for the cubic phase for which most theoretical calculations have been made. This result might be anticipated for γ from the fact that the atomic volumes of the two phases are equal. The value of θ_o is in good agree-

ment with that calculated from elastic constants. The value of γ is discussed below, along with the γ values of the other alkali metals.

2. Electronic Heat Capacity

The values of γ, the coefficient of the linear term in the heat capacity, have been obtained as described in the previous section (B), and are collected in Table IX. Robert's experimental data for lithium are included, as well as certain theoretical predictions.[9]

The electronic heat capacity is determined by $N(E_F)$, the density of states at the Fermi surface.

$$N(E_F) = \frac{1}{8\pi^3} \iint \frac{dS}{|\mathrm{grad}_k E|}, \qquad (6)$$

in which dS is the element of surface, E the energy, k the wave vector, and the integration is extended over the Fermi surface. The thermal effective mass ratio, m^*_t/m, is defined by $m^*_t/m = \gamma/\gamma_f$ where γ_f is the value of γ for free electrons at the density that exists in the metal. This ratio is thus a measure of the difference between the actual density of states at the Fermi surface and that which would be obtained for free electrons.

Theoretical calculations of the electronic structure of metals usually treat separately the various contributions to the departure of the effective mass ratio from unity. These contributions are: (a) the periodic field of the ions at the lattice sites, (b) the electron-electron interactions, and (c) the electron-phonon interactions.

The lattice field has been treated by a number of authors in varying degrees of approximation. The most exact calculations are those made by Brooks and co-workers using the Quantum Defect Method.[36] In

Table IX. Values of the coefficient of the linear term in the heat capacity for lithium, sodium, potassium, rubidium, and cesium.

	Li	Na	K	Rb	Cs
γ (millijoules mole^{-1} deg^{-2})	1.75[a]	1.44	2.11	2.47	3.38
γ_f(millijoules mole^{-1} deg^{-2})[b]	0.745	1.091	1.669	1.907	2.233
$m_t^*/m = \gamma/\gamma_f$	2.35	1.32	1.26	1.30	1.51
m^*/m (Band theory)[c]	1.40	0.98	0.94	0.87	0.83
m^*/m (Electron-electron interactions)[d]	0.84	0.90	0.93	0.95	0.96
m^*/m (Electron-phonon interactions)[e]	2.25	1.35	1.26	1.40	1.51
m^*/m (Electron-phonon interactions)[f]	1.35	1.45	1.59	1.61	1.69

[a] Experimental value taken from Roberts (Ref. 9).

[b] Calculated from Eq. (5). To determine the atomic volume, the lattice constant measured at 78 °K by Barrett (Ref. 8) was used for lithium, and the lattice constants measured at 5 °K by Barrett were used for sodium, potassium, rubidium, and cesium.

[c] Calculated by Brooks (Ref. 14), using the Quantum Defect Method.

[d] Pines (Ref. 16).

[e] Calculated from the theory of Buckingham and Schafroth (Ref. 17). Their factor $(1/2)^{1/3}F$ was calculated from Frohlich's (Ref. 35) Eq. (6.4) and Eq. (6.5) using resistivity values taken from the Handbook of Chemistry and Physics, 34th. Ed. (Chemical Rubber Publishing Company, Cleveland, Ohio, 1952), pp. 2186-2191. It should be pointed out that Frohlich's Eq. (6.5) is in error and that his value for D should be divided by 2.

[f] J.J. Quinn, The Fermi Surface, edited by W.A. Harrison and M.B. Webb (John Wiley & Sons, Inc. New York, 1960), p. 63.

this method, the lowest state of the band is found by a cellular calculation in which a single conduction electron moves in the potential of an ion core located at the center of the unit cell. The potential is taken to be that of the free atom and the energy is obtained by comparing free-atom wave functions of known energy (the atomic energy level) with wave functions satisfying the appropriate boundary conditions (zero normal derivative) over the surface of the unit cell. The higher energy levels are obtained only to terms in k^2. The resulting E vs k relationship is characterized by a single parameter, which may be taken as m^*/m. The values, shown in Table IX, should be compared with m^*_t/m only if the parabolic dependence of E on k continues up to the Fermi energy. For large k values the surfaces of constant energy may become anisotropic, in which case the Fermi surface will develop bulges. There will then be an increase in the density of states and in m^*_t/m, as long as the Fermi surface does not actually touch the zone face. If it does touch, there may be a decrease resulting from the decrease in area of the Fermi surface. A considerable body of theoretical and experimental evidence exists that for sodium and potassium the Fermi surface is close to spherical, but that for other alkali metals it is appreciably distorted, and that it may touch in cesium, and probably does touch in lithium.[15]

A spherical shape for the Fermi surface in sodium and potassium is suggested by a qualitative estimate of the size of the energy gaps at the boundary of the first Brillouin zone[15] and by the temperature dependence of the thermoelectric power.[37] The most direct evidence bearing on this point is the cyclotron resonance experiment on potassium by Kip and Grimes, in which the cyclotron frequency was found to vary by only 4% as the orientation of the sample was changed.[38] In view of this

evidence that the Fermi surface is approximately spherical in sodium and potassium, it is reasonable to compare the observed m^*_t/m with Brooks' values for m^*_t/m. In each case the experimental value is approximately 30% higher, and the difference can be taken as a measure of the effects of the electron-electron and the electron-phonon interactions. In the case of sodium, this conclusion depends on the assumption that the cubic and hexagonal phases have the same γ values. If we assume that the effects of electron-electron interactions and electron-phonon interactions can be treated separately in these metals, the experimental m^*_t/m values must be considered to be in reasonable agreement with the theoretical predictions. For example, if the contributions to the effective-mass ratio of the three effects are simply added together, the results agree with the experimental value within 10% for most combinations. Of the two calculations of the electron-phonon interaction, that of Quinn gives almost exact agreement for sodium, while that of Buckingham and Schafroth gives the better agreement for potassium.

For potassium, the value of m^*_t/m can be compared with the preliminary results of cyclotron resonance[38] and de Haas van Alphen[39] experiments which give, for the former, 1.25 and 1.30 for difference directions, and, for the latter, 0.9 for a single unknown direction. One might tentatively conclude that the electron-electron and the electron-phonon interactions affect the heat capacity and cyclotron resonance frequencies in the same way, and the de Haas van Alphen period in a different way. It will be of considerable interest to compare the results with the complete cyclotron resonance data and the de Haas van Alphen data when they become available.

For rubidium and cesium, the uncertainty in the shape of the Fermi

surface makes a comparison of the m^*_t/m ratio with theory much less meaningful, although in fact the agreement is comparable to that obtained for sodium and potassium. Presumably, cyclotron resonance and other experiments relating to the geometry of the Fermi surface will be extended to these metals in the future, and then the heat-capacity data will be useful in determining the role of electron-electron and electron-phonon interactions.

3. Lattice Heat Capacity

The lattice heat capacities of potassium, rubidium, and cesium are shown in Figs. 11, 12, and 13 as plots of effective Debye temperature θ, vs T. The $\theta(T)$ is defined by equating $C-\gamma T$ to the Debye heat-capacity function. Beattie's table of the Debye heat-capacity function was used.[40] In the liquid helium region, the individual heat-capacity points were used. In addition, a smooth curve is given which is in each case the equivalent of the straight line used to fit the plots of $(C-\gamma T)/T^3$ vs T^2 at lower temperatures. Figure 14 shows smooth curves of θ/θ_0 vs T/θ_0 for potassium, rubidium, and cesium, together with smoothed points obtained by other workers at higher temperatures.

De Launay has given expressions for the T^3 and T^5 terms in the lattice heat capacity for cubic metals.[21] The model used assumed central forces between first and second neighbors, together with a volume force representing the contribution of the conduction electrons. The three parameters introduced are determined in terms of the independent elastic constants for cubic crystals, and tables are given permitting evaluation of coefficients A and B in Eq. (2) in terms of these constants. De Launay distringuishes two cases: Case I, in which the contribution of the electrons to the elastic constants is assumed not

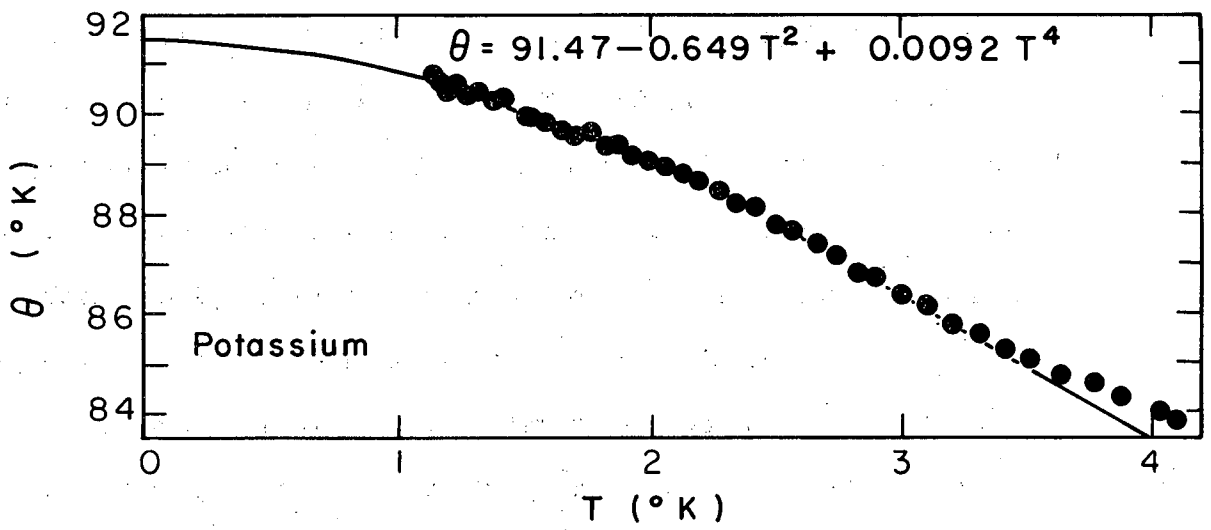

MU-25005

Fig. 11. θ vs T for potassium.

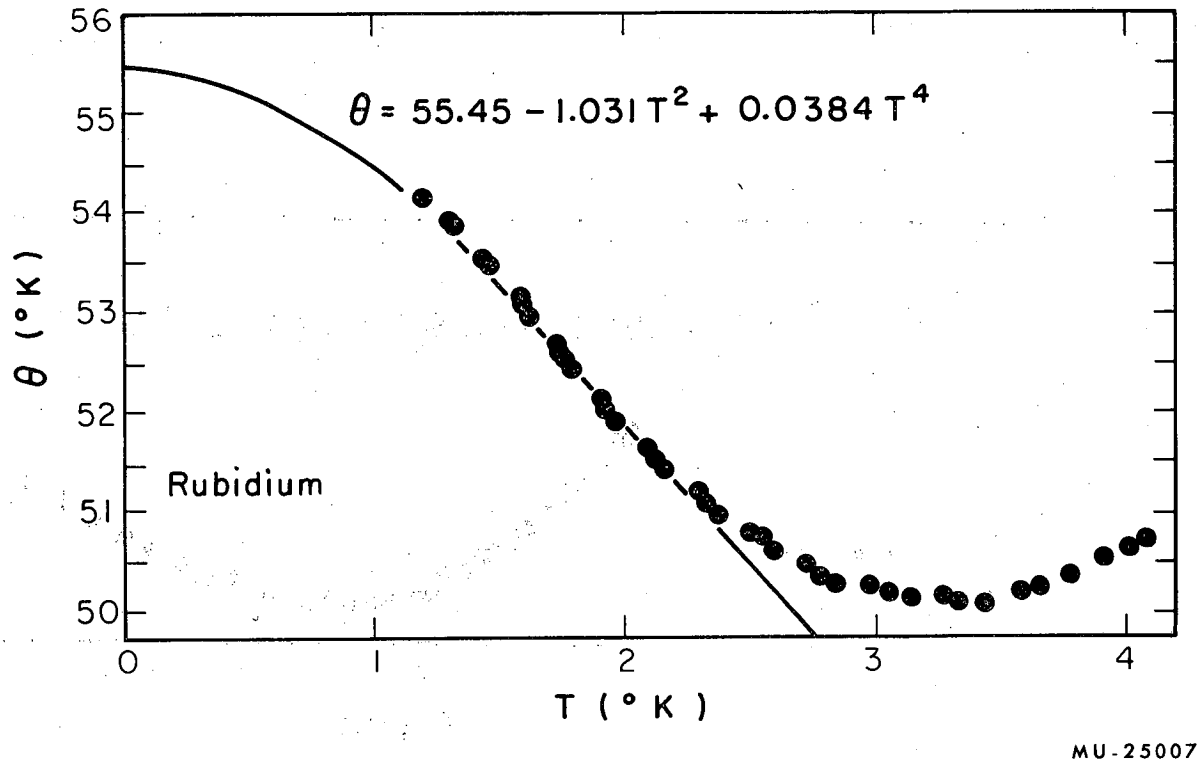

Fig. 12. θ vs T for rubidium.

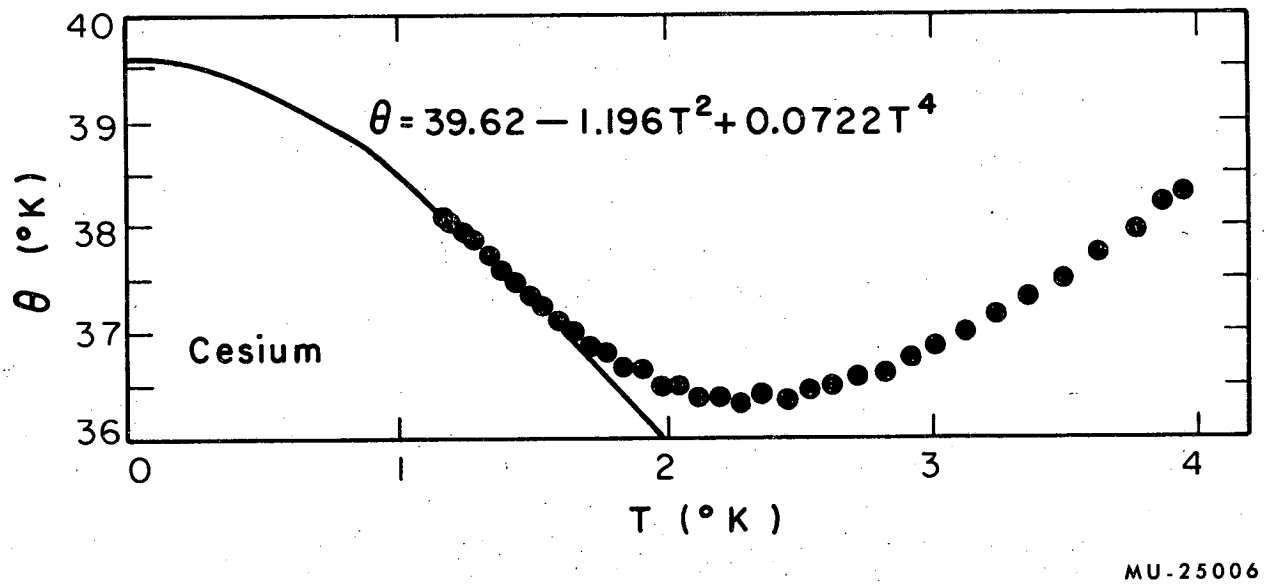

Fig. 13. θ vs T for cesium.

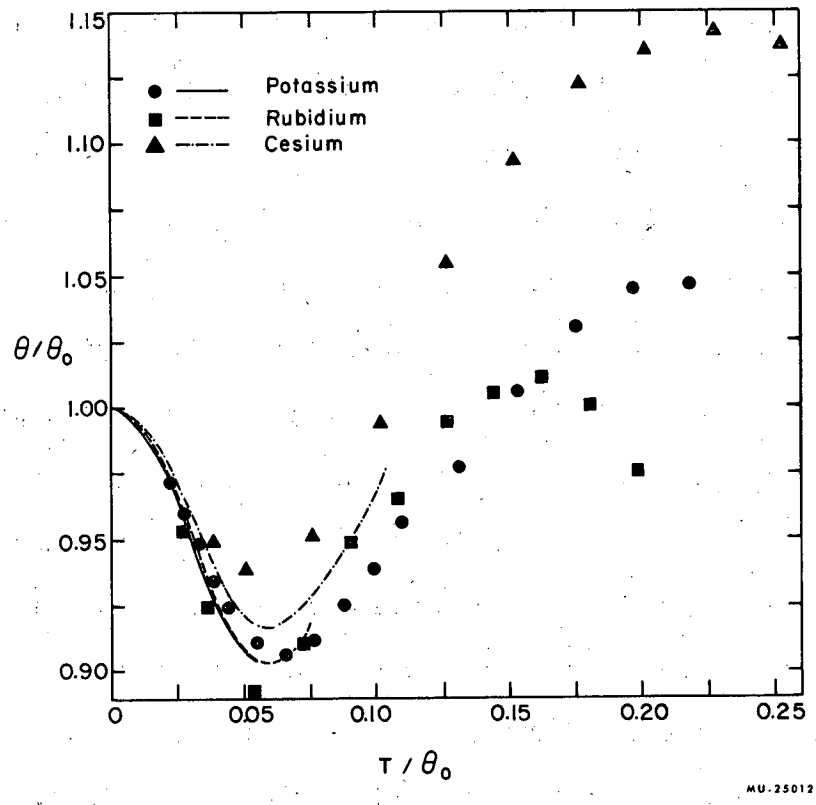

Fig. 14 θ/θ_0 vs T/θ_0 for potassium, rubidium, and cesium. The circles were calculated from the data of Roberts (Ref. 9). The squares and triangles were calculated from the data of McCollum (Ref. 33).

to contribute to the restoring forces involved in thermal excitation, and Case II, in which it is assumed that the electrons follow the thermal vibrations of the lattice. The heat capacity calculated in the two cases is not very different, presumably because the longitudinal vibrations, the only ones affected by the bulk modulus of the electron gas, make only a minor contribution to the low-temperature heat capacity. It seems evident that for the lowest frequency modes that determine the T^3 term the electrons must follow the motion of the ions, and therefore Case II must apply. On that assumption, θ_0 is related to the elastic constants as in the Debye continuum theory, and the agreement generally found between calorimetric and elastic constants data does not confirm the validity of the model. At slightly higher temperatures where dispersion introduces the T^5 terms the theory has not been tested, because for most cubic metals the T^5 term is important only above 4 °K where there are no heat-capacity data available, and the theory has also not been applied to any non-cubic metals for which some data are available. The coefficients of the T^3 and T^5 terms in the lattice heat capacity are compared with de Launay's calculations in Table X. For potassium, rubidium, and cesium, only approximate values of the elastic constants are available, and the ones used in the comparison were taken from the compilation by Huntington.[41] The atomic volumes used in the calculation were taken from Barrett's low-temperature x-ray data.[8] In this table, f' is a parameter introduced by de Launay and is given by:

$$C = \frac{12}{5} \pi^4 R \left[\left(\frac{T}{\theta_0}\right)^3 + f' \left(\frac{T}{\theta_0}\right)^5 \right] \qquad (7)$$

The discrepancy between the calorimetric and elastic constants data for the θ_0's of rubidium and cesium probably reflects the error in the

Table X. Comparison of the T^3 and T^5 terms in the lattice heat capacity derived from this work, with de Launay's results.

	$A\left(\frac{\text{millijoules}}{\text{mole}^{-1}\ \text{deg}^{-4}}\right)$	$\theta_0(^\circ K)$	$B\left(\frac{\text{millijoules}}{\text{mole}^{-1}\ \text{deg}^{-6}}\right)$	f'	
K	2.540	91.5	0.0540	178	This work
K	2.438	92.7	0.0262	92	de Launay
Rb	11.40	55.5	0.636	172	This work
Rb	14.44	51.3	0.577	105	de Launay
Cs	31.25	39.6	2.83	142	This work
Cs	33.81	38.6	2.33	103	de Launay

calculated elastic constants. For potassium, the elastic constants were measured at 77 ^{o}K and extrapolated to 0 ^{o}K, and the agreement is reasonable.

The observed coefficient of the T^5 term is in poor agreement with theory. For potassium, the comparison is clear: the elastic constants are relatively well known and predict θ_0 accurately, but there is a disagreement by a factor of two in B. For rubidium and cesium the elastic constants are less certain, and it is not clear whether comparison should be made on the basis of B or f′, but in either case the disagreement is significant. The difference between the calculated and observed T^5 terms is probably caused by the inadequacy of a model that includes only second-neighbor interactions. Dispersion curves obtained by neutron diffraction techniques have also required the inclusion of more than second-neighbor interactions.

D. Conclusion

It can be said that the present theoretical treatment of the electron-electron and electron-phonon interactions in the alkali metals are in qualitative agreement with the observed electronic heat capacity, if it is assumed that those effects can be treated separately. The principal additional uncertainties in this interpretation are associated with the lack of detailed information about the shape of the Fermi surface in lithium, rubidium, and cesium, and with the validity of the models on which the various theoretical treatments are based. The observed lattice heat capacity is not in agreement with de Launay's calculations, presumably because a model employing only first- and second-neighbor interactions is inadequate.

PART II: SMALL PARTICLES OF MAGNESIUM OXIDE

I. HEAT CAPACITY OF SMALL PARTICLES OF MAGNESIUM OXIDE

A. Introduction

For most purposes, the thermodynamic properties of solids can be assumed to be proportional to volume. For very small particles, however, this assumption must break down, and in recent years there has been both theoretical and experimental interest in surface contributions to thermodynamic properties. Experimentally, the surface contributions to thermodynamic properties can be determined by measuring the heat capacity of a material with a large specific surface area and comparing this with the heat capacity of a macrocrystalline sample of the same material.

The theory discussed below shows that even for the smallest obtainable particles an appreciable effect on heat capacities would be found only at liquid helium temperatures. Because of the large surface area of the samples it would be impossible to use helium-exchange gas, and without exchange gas long thermal equilibrium times could be expected. In an apparatus of the mechanical switch variety already described (Sec. I-B of Part I), in which the residual heat leak is very small, long equilibrium times could be tolerated. A preliminary experiment was carried out to determine the time necessary for thermal equilibrium without exchange gas. Heat was introduced into the interior of a loosely packed, thermally isolated sample of magnesium oxide powder at liquid helium temperatures. The temperature changes at the surface of the sample were observed. The surface temperature followed changes in heater power with a time lag of approximately 5 minutes showing the feasibility of heat-capacity measurements at these temperatures.

Heat-capacity measurements were then made on two samples of magnesium oxide with specific surface areas of 166 m^2/g and 13.1 m^2/g. Magnesium oxide was chosen, partly because of its ease of preparation, and partly because measurements at higher temperatures by Giauque and Archibald suggested that a large surface contribution would be found at liquid helium temperatures.[42]

Three theoretical investigations have been made on this problem. Montroll[43] and Dupuis[44] both calculated the contribution to the heat capacity of the surface for particle sizes and temperatures at which an elastic continuum model is valid. Jura and Pitzer discussed a contribution to the heat capacity by the external movements of the small particles, and also pointed out that for very small particles the breakdown of the elastic continuum approximation becomes of practical importance.[45]

Montroll treats the case of an elastic solid on the assumption that the surfaces are perfectly reflecting. This simplification makes possible an analysis of the modes of vibration in terms of pure-longitudinal and pure-transverse acoustical waves. He used the frequency spectrum calculated by Bolt and Maa, which contains a term proportional to the surface area and the first power of the frequency in addition to the usual term proportional to the volume and the second power of the frequency.[46] Therefore in addition to the usual Debye T^3 term in the heat capacity, there is also a T^2 term that is proportional to the surface area. For the case of very small particles, a term in the heat capacity proportional to T and to the total length of the edges of the particles becomes important. The volume-dependent term is

$$C_v = 96\pi \frac{k^4}{h^3} \zeta(4) \left(\frac{1}{c_\ell^3} + \frac{2}{c_t^3}\right) V T^3 = \frac{12}{5} \pi^4 R \left(\frac{T}{\theta}\right)^3 , \qquad (8)$$

where $\zeta(4)$ is the Rieman zeta function of argument 4, C_ℓ the longitudinal sound velocity, C_t the transverse sound velocity, V the molar volume, R the gas constant, and θ the Debye characteristic temperature.

The surface-dependent term is

$$C_S = 3\pi \frac{k^3}{h^2} \zeta(3) \left(\frac{1}{C_\ell^{\,2}} + \frac{2}{C_t^{\,2}} \right) S\, T^2 , \tag{9}$$

where S is the total surface area. The edge-dependent term is

$$C_{edge} = \frac{1}{4} \frac{k^2}{h} \zeta(2) \left(\frac{1}{C_\ell} + \frac{2}{C_t} \right) L\, T , \tag{10}$$

where L is the total elngth of the edges.

Dupuis computed the surface specific heat of an isotropic solid for the case of stress-free surfaces, so that the normal modes of vibration are neither pure-transverse nor pure-longitudinal waves, as this type of surface "scatters" and mixes the waves. He points out that this type of surface is physically realistic in contrast to that considered by Montroll. He calculated a surface specific heat with the same surface area and temperature dependence as Montroll's, but with a coefficient approximately 50% larger. Dupuis interprets his result by saying that the surface contribution arises from the energy associated with Rayleigh surface waves, and from the phase shift of the waves at the boundaries. His equation for the surface heat capacity is

$$C_S = 3\pi \frac{k^3}{h^2} \zeta(3) \frac{2C_t^4 - 3C_t^2 C_\ell^2 + 3C_\ell^4}{C_t^2 C_\ell^2 (C_\ell^2 - C_t^2)} S\, T^2 \tag{11}$$

Dupuis' result should hold as long as ℓ_3, the smallest dimension of the particle, is not too small. From the approximations made in his calculations, $4\pi\ell_3 T/\hbar C_\ell$ must be greater than 10. For magnesium oxide then,

ℓ_3 T must be greater than 6×10^{-6} cm-deg, or 600 A at 1°K.

Jura and Pitzer have pointed out that for very small particles some long-wave-length normal modes are eliminated from the frequency spectrum, with a consequent reduction in heat capacity associated with the internal degrees of freedom. At temperatures low compared with θ, the lattice vibrations contributing most to the heat capacity of a solid have a wave length of the order of $a\theta/T$, where a is the lattice constant. For magnesium oxide, it follows that at liquid helium temperatures the volume-dependent part of the heat capacity of particles with linear dimensions of 1000 A or less is less than that of macrocrystalline samples of the same material. This also means that heat-capacity calculations on particles smaller than 1000 A must sum over all possible modes of vibration, rather than making use of a continuous frequency spectrum. Jura and Pitzer also show that the heat capacity associated with the external motion of the particles can be important. They treat these motions as behaving classically to give a constant heat capacity contribution of 6 k per particle. They have calculated the heat capacity of a material with a Debye characteristic temperature of 400 ^{o}K, and which is in the form of cubes measuring 100 A on an edge. The bulk elastic constants were used in calculating the frequencies associated with the internal degrees of freedom. The two terms in the heat capacity are of comparable size at 3 ^{o}K, but the constant term dominates below 1.5 ^{o}K. As the particles become larger, the contribution of the gross motion becomes smaller. However, their calculations shown an appreciable effect of particle size up to cubes 600 A on an edge. The effect becomes especially marked as the cube edge becomes less than 200 A.

B. Results

The first sample of magnesium oxide on which heat-capacity measurements were made had a specific surface area of 166 m^2/g, as determined by nitrogen adsorption isotherms at 77 ^oK. This surface area corresponds to an edge length of 101 A, assuming that the particles are cube shaped. The sample was prepared by dehydration at 350 ^oC of laboratory-prepared magnesium hydroxide. The powder had an average density of 0.72 g/cm^3, compared with the crystal density of magnesium oxide of 3.58 g/cm^3. A 62.51 g sample was placed in a calorimeter constructed from 0.002-in. copper. The calorimeter was a 1 1/2-in.-diam/cylinder 3 1/4 in. high, and containing copper vanes to enhance the heat transfer between the heater and the powder. It weighed 15.03 g, and was mostly copper. The heat capacity of the empty calorimeter was also measured, and graphic means were used to subtract its heat capacity from the total.

The second sample measured had a specific surface area of 13.1 m^2/g, which corresponds to an edge length of 1280 A. It was Baker and Adamson reagent special, magnesium oxide powder. It had an average density of 0.52 g/cm^3. A 94.85 g sample was placed in a calorimeter constructed from 0.001-in. copper. The calorimeter was a cylinder of 1 7/8 in. in diam, and was 6 in. high, and also contained copper vanes. It weighed 10.74 g, and was mostly copper. Its heat capacity was also measured separately, and graphic means were used to subtract its heat capacity from the total.

The experimental values for the 166 m^2/g sample are given in Table XI, and those for the 13.1 m^2/g sample in Table XII. The heat capacity of the empty calorimeter was approximately 40% of the total in both experiments.

Table XI. Heat capacities of magnesium oxide with a specific surface area of 166 m^2/g. Values are in millijoules $mole^{-1}$ deg^{-1}.

T	C	T	C
1.612	0.4627	1.431	0.3053
1.717	0.4675	1.587	0.3840
1.850	0.5700	1.707	0.4806
2.430	1.008	1.774	0.5384
2.628	1.213	1.858	0.5978
2.860	1.469	1.968	0.6557
3.084	1.640	2.091	0.7286
3.388	2.002	2.180	0.8098
3.785	2.627	2.336	0.9620
4.188	3.194	2.586	1.168
		2.753	1.340
		2.895	1.565
		3.084	1.684

Table XII. Heat capacities of magnesium oxide with a specific surface area of 13.1 m^2/g. Values are in millijoules $mole^{-1}$ deg^{-1}.

T	C	T	C
1.315	0.0814	2.724	0.4745
1.371	0.1280	2.684	0.4531
1.410	0.1517	2.226	0.3238
1.819	0.2244	2.341	0.3661
1.932	0.2318	2.458	0.3921
1.267	0.0841	2.674	0.4498
1.335	0.1022	2.916	0.5732
1.396	0.1070	3.135	0.6826
1.525	0.1578	3.355	0.7819
1.559	0.1441	3.504	0.8565
1.819	0.2061	3.794	1.039
1.853	0.2116	2.971	0.5769
2.099	0.2728	3.176	0.7082
2.177	0.2777	3.411	0.7901
2.161	0.2809	3.666	0.9676
2.282	0.3051	3.923	1.207
2.664	0.4616		

Figure 15 shows the heat capacity of 166 m^2/g sample as a plot of C/T^3 vs T. This plot emphasizes the difference between the small and macroscopic crystals, for which C/T^3 would be constant over this temperature range and equal to 0.00459 millijoules per $mole^{-1}$ deg^{-4}. This value is from the heat-capacity measurements of Barron, Berg and Morrison,[47] and from it they calculate a value of 946 ^oK for the Debye characteristic temperature of magnesium oxide.

Figure 16 shows the heat capacity of both samples as plots of C/T^2 vs T. These plots indicate for both samples that the data can be represented reasonably well by a T^2 term plus a T^3 term. Using 0.0046 millijoules $mole^{-1}$ deg^{-4} as the coefficient of the T^3 term, a line of that slope was fitted to both sets of points. The intercepts of these lines then determined the coefficients of the T^2 terms. Thus the data for the 166 m^2/g sample can be represented by $C = 0.163T^2 + 0.0046T^3$ millijoules $mole^{-1}$ deg^{-1}, and the data for the 13.1 m^2/g sample by $C = 0.054T^2 + 0.0046T^3$ millijoules $mole^{-1}$ deg^{-1}. However, in view of the limited range of temperature over which these measurements have been made, and the relatively low precision, this analysis of the data must not be considered unique, particularly for the 166 m^2/g sample.

Because of the long equilibrium times (approx 5 min) involved in these measurements, and to the rather small total heat capacity, the accuracy is not nearly so good as in the case of the measurements on the alkali metals reported in Sec. II of Part I. An estimated upper limit of 10% error is placed on the over-all accuracy of the measurements.

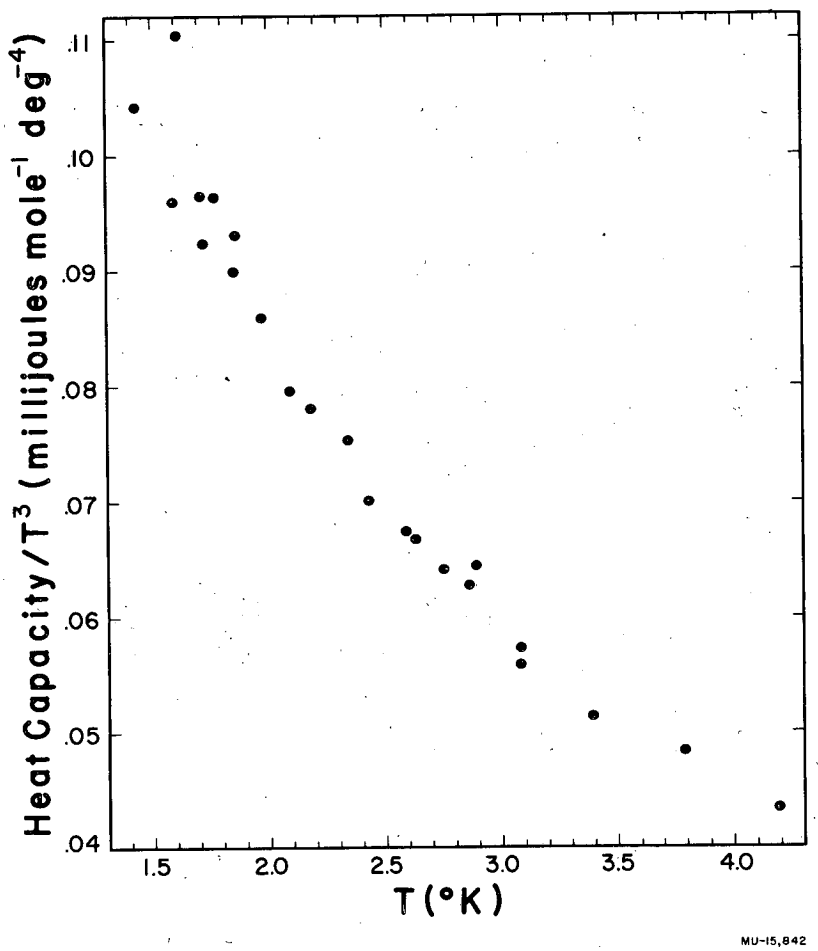

Fig. 15. C/T^3 vs T for magnesium oxide, with a specific surface area of 166 m^2/g.

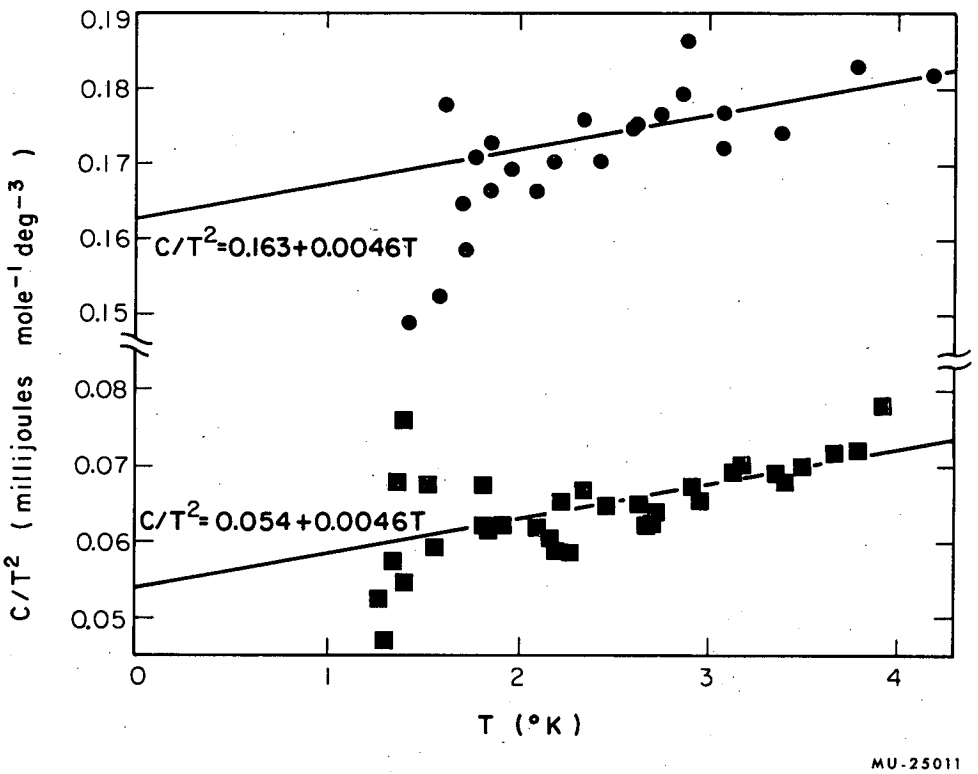

Fig. 16. C/T^2 vs T for both samples of magnesium oxide. Circles represent the 166 m^2/g sample. Squares represent the 13.1 m^2/g sample.

The thermal conductivity of the 166 m^2/g sample, as estimated from the thermal equilibrium times, is about 5×10^{-8} w cm^{-1} deg^{-1}. This value is considerably larger than had been expected on the basis of what is known about heat transfer between macroscopic surfaces and indicates the possibility that motion of the individual particles may have contributed to heat transport.

C. Discussion

On the assumption that the 166 m^2/g sample of magnesium oxide consists of perfect cubes, we find that the edge length is 101 A and that there are 1.09×10^{19} particles per mole. At 6 k per particle, this means that there should be a constant term in its heat capacity of 0.906 millijoules $mole^{-1}$ deg^{-1}. However, Table XI shows that the heat capacity is smaller than this at 2 ^{o}K and continues to decrease with temperature. Also, Fig. 16 shows that the data are represented reasonably well by a T^2 and T^3 term, so it appears that the constant term in this case is less than one-tenth of that calculated. A very plausible reason for this discrepancy is that the particles are not perfect cubes but have rough surfaces and cracks or fissures that add to the surface area and therefore lead to an overestimate of the number of particles. An electron microscope examination showed clusters of 200 A diam/ particles, but it was impossible to determine whether or not they were truly independent units. X-ray diffraction-line broadening indicated a particle size of 71 A.

If we take for average sound velocities in magnesium oxide the values computed by Dupuis, and use Eq. (11), the surface heat capacity is 6.46×10^{-6} S T^2 ergs $mole^{-1}$ deg^{-1}, where S is the surface area in

cm^2/mole.

For the 166 m^2/g sample, the computed surface heat capacity is 0.043 T^2 millijoules $mole^{-1}$ deg^{-1}, as compared with 0.163 T^2 millijoules $mole^{-1}$ deg^{-1} taken from Fig. 16. Of course, particles of 101 A at liquid helium temperatures are clearly smaller than the lower limit Dupuis has established for the validity of his theory, so the disagreement is not surprising. Also, for particles this small, edge corrections should be important and Eq. (9) gives a contribution of 0.068 T^2 millijoules $mole^{-1}$ deg^{-1} to the heat capacity, but this is not observed.

For the 13.1 m^2/g sample, the computed surface heat capacity is 0.0034 T^2 millijoules $mole^{-1}$ deg^{-1}, as compared with 0.054 T^2 millijoules $mole^{-1}$ deg^{-1} taken from Fig. 16. This discrepancy of a factor of 16 seems far outside the limit of error of the heat-capacity measurements and the uncertainties in the data analysis. Again, however, the fact that the surface is rough and made up of cracks or fissures in the particles might lead to a very different surface heat capacity than that computed by Dupuis for a plane surface.

A factor that could be important in explaining the discrepancies between experiment and theory for surface-heat capacities of small particles is that the theories have used the macroscopic elastic constants in their calculation of the frequencies of small-particle modes of vibration. In light of Dupuis' result that Rayleigh surface waves are an important contribution to the surface energy, and since the restoring forces acting on atoms on the surface would be smaller than those acting on atoms in the interior, it seems that the use of macroscopic elastic constants would give a low estimate of the surface heat capacity.

Related to this effect is the possibility that the surface is chemically different from the interior, which would also change its elastic properties. The tendency of magnesium oxide to adsorb water makes it a poor choice for experimental work for this reason. The 166 m^2/g sample contained a total of 6% water; no analysis was made on the 13.1 m^2/g sample.

In summary, these experiments demonstrate the feasibility of investigating the heat capacity of small particles, but an adequate test of the models involved in the calculations will require measurements on regularly shaped particles with uniform chemical composition, over a wider range of temperatures.

ACKNOWLEDGMENTS

The author wishes to express his sincere appreciation for the inspiring guidance of Professor Norman E. Phillips whose advice, encouragement and unbounded interest provided a large contribution toward the completion of this work.

This work was performed under the auspices of the U.S. Atomic Energy Commission.

APPENDIX. Heat-Capacity Anomaly in Solid Air

The heat capacity of the air is shown in Fig. 17. There is an uncertainty of perhaps 5% in the amount of air present, and therefore in the values plotted in the figure. In this temperature range, the heat capacity of solid air is as much as 400 times as great as that of solid oxygen.[48]

It seems probable that the large heat capacity is associated with an antiferromagnetic ordering of the electron spins of the oxygen molecules at about 3 °K. From a comparison of the spectroscopic entropy of oxygen gas with calorimetric measurements on the condensed phases, Giauque and Johnston showed that in pure solid oxygen the spins are largely aligned at liquid hydrogen temperatures.[49] Calorimetric[49,50] and magnetic[50,51] susceptibility data suggest that a tranformation to an antiferromagnetic state is coincident with the γ-β crystallographic transition at 43.8 °K. Dilution of an antiferromagnet with a diamagnetic material reduces the energy of interaction between the spins. Consequently, the alignment of the spins in solid air can be expected to take place at a lower temperature than in pure oxygen. Further support for this point of view comes from magnetic susceptibility measurements on liquid oxygen-nitrogen solutions. Between 64 and 77 °K these solutions follow a Curie-Weiss law with antiferromagnetic Weiss constants.[52] The Weiss constant for a composition corresponding to the present sample would be about 7 °K, within the usual range of values that might be expected for a material with a Neel temperature of 3 °K. The fact that the heat capacity does not exhibit the λ-anomaly characteristic of antiferromagnetic transitions in pure compounds is to be

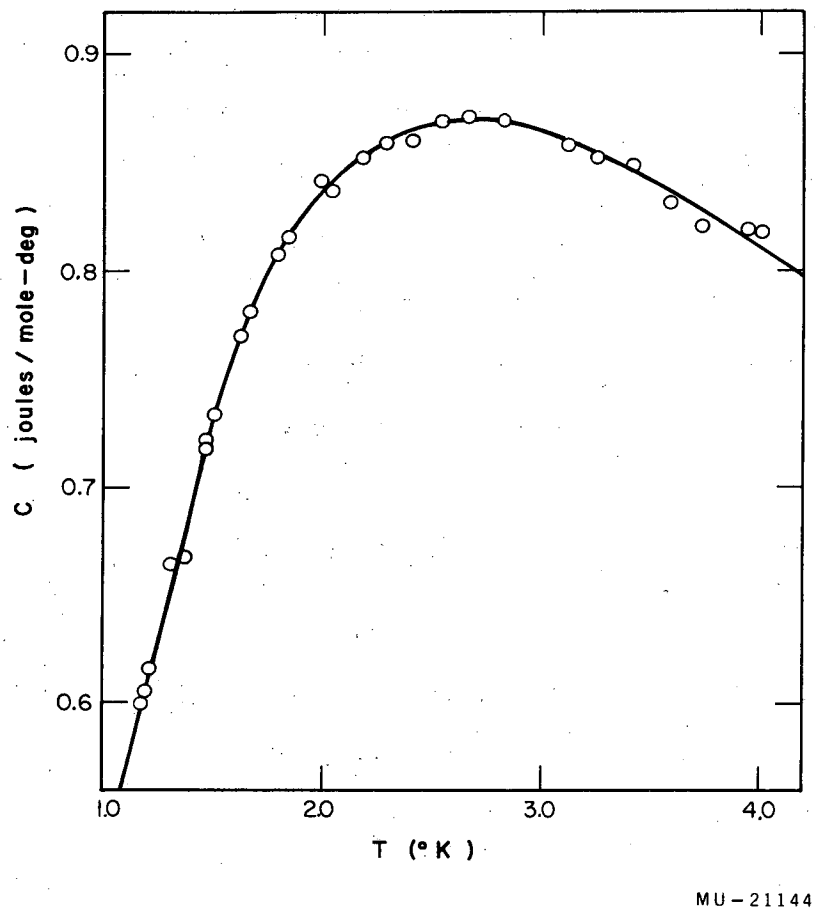

Fig. 17. The heat capacity of solid air.

expected on general grounds, and also by comparison with magnetic susceptibility measurements on solutions which show a broadening of the antiferromagnetic transition.[53]

REFERENCES

1. W. Nernst, Ann. Physik 36, 395 (1911).
2. A. Eucken, Physik. Z. 10, 586 (1909).
3. J. C. Wheatley, D. F. Griffing, and T. L. Estle, Rev. Sci. Instr. 27, 1070 (1956).
4. H. van Dijk and M. Durieux, Progress in Low Temperature Physics, Vol. 2 (North-Holland Publishing Company, Amsterdam, 1957), pp. 461-462.
5. F. G. Brickwedde, H. Van Dijk, M. Durieux, J. R. Clement and J. K. Logan, J. Research Natl. Bur. Standards 64A, 1 (1960).
6. H. S. Sommers, Jr., Rev. Sci. Instr. 25, 793 (1954).
7. R. A. Erickson, L. D. Roberts, and J. W. T. Dabbs, Rev. Sci. Instr. 25, 1178 (1954).
8. C. S. Barrett, Acta Cryst. 9, 671 (1956).
9. L. M. Roberts, Proc. Phys. Soc. (London) B70, 744 (1957).
10. J. Rayne, Phys. Rev. 95, 1428 (1954).
11. A. Sommerfeld, Z. Physik, 47, 1 (1928).
12. F. Bloch, Z. Physik, 52, 555 (1928).
13. C. Kittel, Introduction to Solid State Physics (John Wiley and Sons, Inc., New York, 1956), p. 291.
14. H. Brooks, quoted in C. Kittel, Introduction to Solid State Physics (John Wiley and Sons, Inc., New York, 1956), p. 317.
15. M. H. Cohen and V. Heine, Advances in Physics 7, 396 (1958).
16. D. Pines, Solid State Physics, Vol. 1 (Academic Press, Inc., New York, 1955), p. 367.
17. M. J. Buckingham and M. R. Schafroth, Proc. Phys. Soc. (London) A67, 828 (1954).

18. P. Debye, Ann. Physik, 39, 789 (1912).

19. M. Blackman, Proc. Roy. Soc. (London) A159, 416 (1937).

20. M. Blackman, Rep. Progr. Phys. 8, 11 (1941).

21. J. Launay, Solid State Physics, Vol. 2 (Academic Press Inc., New York, 1956), pp. 219-303.

22. W. S. Corak, B. B. Goodman, C. B. Satterthwaitte, and A. Wexler, Phys. Rev. 98, 1699 (1955).

23. J. Rayne, Australian J. Phys. 9, 189 (1956).

24. G. Kneip, private communication.

25. N. E. Phillips, (Lawrence Radiation Laboratory, Berkeley) private communication.

26. D. H. Parkinson and J. E. Quarrington, Brit. J. Appl. Phys. 5, 219 (1954).

27. N. E. Phillips, Phys. Rev. 114, 676 (1959).

28. C. G. B. Garrett, Proc. Roy. Soc. (London) A203, 375 (1950).

29. N. E. Phillips, Phys. Rev. Letters 1, 363 (1958).

30. N. E. Phillips, to be published.

31. A. H. Cooke, H. Meyer, and W. P. Wolf, Proc. Roy. Soc. (London) A233, 536 (1956).

32. D. L. Martin, Phys. Rev. (to be published).

33. D. C. McCollum, Low-Temperature Specific Heats of Rubidium and Cesium, (Ph.D. Thesis), Physics Department, University of California, Berkeley, 1960.

34. F. D. Manchester, Can. J. Phys. 37, 525 (1959).

35. H. Frohlich, Phys. Rev. 79, 845 (1950).

36. The Quantum Defect Method has been reviewed by F. S. Ham, in Solid State Physics, Vol 1 (Academic Press, Inc., New York, 1955) p. 127.

37. D. K. C. McDonald, W. B. Pearson, and J. M. Templeton, Proc. Roy. Soc. (London) A256, 334 (1960).

38. A. F. Kip and C. Grimes (Physics Department, University of California),private communication.

39. A. C. Thorsen and T. G. Berlincourt, Phys. Rev. Letters 6, 617 (1961).

40. J. A. Beattie, J. Math and Phys. 6, 1 (1926).

41. H. B. Huntington, in Solid State Physics, Vol. 7 (Academic Press, Inc., New York, 1958) p. 288.

42. W. F. Giauque and R. C. Archibald, J. Am. Chem. Soc. 59, 561 (1937).

43. E. W. Montroll, J. Chem. Phys. 18, 183 (1950).

44. Marc Dupuis, Investigations in the Theory of Solids, (Ph.D. Thesis), Yale University, 1959; and M. Dupuis, R. Mazo, and Lars Onsager, J. Chem. Phys. 33, 1452 (1960).

45. G. Jura and K. Pitzer, J. Am. Chem. Soc. 74, 6030 (1952).

46. R. H. Bolt, J. Acoust. Soc. Am. 10, 228 (1939).

47. T. H. K. Barron, W. T. Berg and J. A. Morrison, Proc. Roy. Soc. (London) A250, 70 (1959).

48. M. O. Kostriukova and P. G. Strelkov, Doklady Akad. Nauk S.S.S.R. 90, 525 (1953).

49. W. F. Giauque and H. L. Johnson, J. Am. Chem. Soc., 51, 2300 (1929).

50. A. S. Borovik-Romanov, M. P. Orlova and P. G. Strelkov, Dokaldy Akad. Nauk S.S.S.R. 99, 699 (1954).

51. E. Kanda, T. Haseda and A. Otsubo, Physica 20, 131 (1954).

52. A. Perrier and H. K. Onnes, Communications from the Physical Laboratory of the University of Leiden, No. 139-d (1914).

53. H. Bizette and B. Tsai, Compt. rend. 217, 444 (1943).

This report was prepared as an account of Government sponsored work. Neither the United States, nor the Commission, nor any person acting on behalf of the Commission:

A. Makes any warranty or representation, expressed or implied, with respect to the accuracy, completeness, or usefulness of the information contained in this report, or that the use of any information, apparatus, method, or process disclosed in this report may not infringe privately owned rights; or

B. Assumes any liabilities with respect to the use of, or for damages resulting from the use of any information, apparatus, method, or process disclosed in this report.

As used in the above, "person acting on behalf of the Commission" includes any employee or contractor of he Commission, or employee of such contractor, to the extent that such employee or contractor of the Commission, or employee of such contractor prepares, disseminates, or provides access to, any information pursuant to his employment or contract with the Commission, or his employment with such contractor.